

Association of S-type and I-type granitoids  
in the Neoproterozoic Cameroon orogenic belt, Bafoussam area,  
West Cameroon: geology, geochemistry and petrogenesis

Dissertation zur Erlangung des  
naturwissenschaftlichen Doktorgrades  
der Bayerischen Julius–Maximilians–Universität Würzburg

vorgelegt von

Merline Laure Djouka-Fonkwé

aus

Nkongsamba, Kamerun

Würzburg 2005

Eingereicht am:

1. Gutachter: [Prof. Dr. U. Schüßler](#)

2. Gutachter: [Prof. Dr. B. Schulz](#)

der Dissertation

1. Prüfer: [Prof. Dr. U. Schüßler](#)

2. Prüfer: [Prof. Dr. H. De Wall](#)

der mündlichen Prüfung

Tag der mündlichen Prüfung: [22. Juli 2005](#)

Doktorurkunde ausgehändigt am:

*In memory of  
Dr. habil. Richard Nana*

**TABLE OF CONTENTS**

<b>ABSTRACT.....</b>	<b>iv</b>
<b>ZUSAMMENFASSUNG.....</b>	<b>vii</b>
<b>ACKNOWLEDGMENTS.....</b>	<b>x</b>
<b>1 INTRODUCTION.....</b>	<b>1</b>
1.1 Geological setting of Cameroon.....	1
1.1.1 Congo craton.....	1
1.1.2. Neoproterozoic orogenic belt .....	6
1.1.2.1 Paleoproterozoic gneissic basement.....	9
1.1.2.2 Late Mesoproterozoic to Neoproterozoic schist belts.....	10
1.1.2.3 Pan-African granitoids.....	12
1.1.2.4 Tectonic evolution of the Neoproterozoic orogenic belt of Cameroon.....	14
1.1.3 Mesozoic to Tertiary sedimentary basins.....	17
1.1.4 Tertiary to recent volcanics.....	18
1.1.4.1 The anorogenic complexes.....	19
1.1.4.2 Volcanism.....	20
1.2 Aim of the study.....	21
<b>2 GEOLOGY OF THE STUDY AREA.....</b>	<b>23</b>
2.1 Metamorphic rocks: migmatic gneiss and amphibolite.....	26
2.2 Granitoid rocks.....	26
2.2.1 Biotite granitoid.....	29
2.2.2 Deformed biotite granitoid.....	30
2.2.3 Mega feldspar granitoid.....	34
2.2.4 Two-mica granitoid.....	37
2.3 Volcanic rocks.....	37
<b>3 PETROGRAPHY.....</b>	<b>40</b>
3.1 Biotite granitoid.....	40
3.2 Deformed biotite granitoid.....	43
3.3 Mega feldspar granitoid.....	49
3.4 Two-mica granitoid.....	52
<b>4 MINERAL CHEMISTRY.....</b>	<b>58</b>
4.1 Micas: biotite and muscovite.....	58
4.1.1 Biotite.....	58
4.1.2 Muscovite.....	63
4.2 Garnet.....	67
4.3 Amphibole.....	70
4.4. Feldspars: potassium feldspar and plagioclase feldspar.....	78
4.4.1 Potassium feldspar.....	78

4.4.2 Plagioclase feldspar.....	80
4.5 Iron-titanium oxides: magnetite and ilmenite.....	80
4.6 Mineral chemistry of igneous phases.....	81
<b>5 ESTIMATES OF CRYSTALLIZATION CONDITIONS.....</b>	<b>83</b>
5.1 Temperature estimates.....	83
5.1.1 Zircon and apatite saturation thermometry.....	83
5.1.2 Hornblende–plagioclase thermometry.....	87
5.2 Pressure estimates.....	89
5.2.1 Aluminium-in-hornblende geobarometry.....	89
5.2.2 Phengite geobarometry.....	92
5.3 Oxygen fugacity estimates.....	93
<b>6 FLUID INCLUSION STUDY.....</b>	<b>97</b>
6.1 Petrography and types of fluid inclusions.....	98
6.1.1 Mixed aqueous–non-aqueous volatile fluid inclusions.....	99
6.1.2 Pure aqueous fluid inclusions.....	100
6.2 Microthermometric data.....	103
6.3 Interpretation and discussion of data.....	106
<b>7 GEOCHEMISTRY.....</b>	<b>110</b>
7.1 Major and trace element geochemistry.....	110
7.1.1 Major elements.....	110
7.1.1.1 Nomenclature of the granitoids.....	112
7.1.1.2 Magmatic affinities.....	115
7.1.2 Trace elements.....	122
7.2 Rare earth element patterns.....	124
7.3 Tectonic setting.....	126
7.4 Genetic type: I-type and/or S-type?.....	132
7.5 Fractional crystallization processes.....	135
<b>8 ISOTOPE CHARACTERISTICS.....</b>	<b>141</b>
8.1 Rubidium–Strontium dating method.....	141
8.2 Samarium–Neodymium dating method.....	143
8.2.1 Epsilon Nd parameter and depleted mantle model ages.....	145
8.3 Combined Nd - and Sr -isotopes and geodynamic implications.....	148
8.3.1 Two components mixing and assimilation – AFC process.....	149
<b>9 DISCUSSION AND CONCLUSIONS.....</b>	<b>155</b>
9.1 Granitoids origin and petrogenesis.....	155
9.1.1 I-type granitoids.....	155
9.1.2 Two-mica granitoid.....	158
9.1.2.1 The peraluminous composition of the two-mica granitoid.....	158
9.1.2.2 Possible source of the two-mica granitoid magma.....	160
9.2 Geodynamic implications.....	163
9.3 Salient results.....	167

---

<b>10 REFERENCES.....</b>	<b>170</b>
<b>APPENDIX.....</b>	<b>A1</b>
A.1 Analytical procedures.....	A1
A.1.1 Petrography.....	A1
A.1.2 Electron microprobe (EMP).....	A1
A.1.3 Whole- rock geochemistry.....	A1
A.1.4 Whole-rock Rb–Sr and Sm–Nd isotope geochemistry.....	A3
A.1.5 Microthermometric fluid inclusion studies.....	A4
A.2 Mineral chemistry.....	A5
A.3 Whole-rock geochemistry.....	A43
A.4 Whole-rock Rb–Sr and Sm–Nd isotope geochemistry.....	A56
A.5 Microthermometric fluid inclusion data .....	A58

**ABSTRACT**

The Bafoussam area in west Cameroon is located within the Cameroon Neoproterozoic orogenic belt (north of the Congo craton) which is part of the Central African Fold Belt (CAFB). The evolution of the CAFB is related to the collision between the convergent West African craton, the São Francisco – Congo cratons and the Sahara Metacraton. The outcrop area stretches over a surface of ~1000 km<sup>2</sup> and dominantly consists of granitoids which intruded wall-rocks of gneiss and migmatite during the Pan-African orogeny. The Bafoussam granitoid emplacement was influenced by the N 30 °E strike-slip shear zone in the prolongation of the Cameroon Volcanic Line, but also by the N 70 °E Central Cameroon Shear Zone. In the field, these two shear directions are expressed in the schistosity and foliation trajectories, fault orientation and the alignment of the volcanic cones as well.

In the Bafoussam area, four types of granitoids can be distinguished, including: (i) the biotite granitoid, (ii) the deformed biotite granitoid, (iii) the mega feldspar granitoid, and (iv) the two-mica granitoid. These granitoids occur as elongated plutons hosting irregular mafic enclaves (amphibole-bearing, biotite-rich, and metagabbroic types) and are frequently cut by late pegmatites, aplite dykes and quartz veins. Petrographically, they range in composition from syenogranite (major), alkali-feldspar granite, granodiorite, monzogranite, quartz-syenite, quartz-monzonite to quartz-monzodiorite. Potassium feldspar, quartz, plagioclase and biotite are the principal phases, in cases accompanied by amphibole and accessory minerals such as apatite, zircon, monazite, titanite, allanite, ilmenite and magnetite. Sericite, epidote and chlorite are secondary minerals. In addition, the two-mica granitoid contains primary muscovite and sometimes igneous garnet.

In the granitoids, potassium feldspar is orthoclase (microcline and orthoclase: Or<sub>81-97</sub>Ab<sub>19-3</sub>), and plagioclase is mainly oligoclase with some albite and andesine (An<sub>3-35</sub>Ab<sub>96-64</sub>). Biotite is Fe-rich (meroxene and lepidomelane, with some siderophyllite), having high Fe<sup>2+</sup>/(Fe<sup>2+</sup> + Mg) ratios of 0.40–0.80. It is a re-equilibrated primary biotite and suggests calc-alkaline and peraluminous nature of the host granitoids. Amphibole is edenitic and magnesian hastingsitic hornblende, with high Mg/(Mg + Fe<sup>2+</sup>) ratios of 0.50–0.62. The evolution of the hornblende was dominated by the edenitic, tschermakitic, pargasitic and hastingsitic substitution types. Primary muscovite is iron-rich [Fe<sup>2+</sup>/(Fe<sup>2+</sup> + Mg) = 0.52–0.82] and has experienced celadonite and paragonite substitutions. Igneous garnet is almandine–spessartine (X<sub>Fe</sub> = 0.99 and X<sub>Mn</sub> = 0.46–0.56). The euhedral grain shapes of garnet crystals and the absence of inclusions coupled with the high Mn and Fe<sup>2+</sup> contents (2.609–3.317 a.p.f.u and 2.646–3.277 a.p.f.u, respectively) and low Mg contents (0.012–0.038 a.p.f.u) clearly point to its plutonic origin. The Mn-depletion crystallization model is suggested for the origin of the analyzed garnet, i.e. initial crystallization of garnet inducing early decrease of Mn in the original melt.

Aluminum-in-hornblende and phengite barometric estimates show that the granitoids crystallized at 4.2 ± 1.1 to 6.6 ± 1.0 kbar, corresponding to emplacement depths of 15–24 km. Zircon and apatite saturation temperature calibrations and hornblende–plagioclase thermometry yielded emplacement temperatures between 772 ± 41 and 808 ± 34 °C. Except the two-mica granitoid, the titanite–magnetite–quartz assemblage gives oxygen fugacities ranging from 10<sup>-17</sup> to 10<sup>-13</sup>, suggesting that the granitoids were produced by an oxidized magma. Since the two-mica granitoid lacks magnetite, it was originated from a magma under reducing conditions, below the quartz–fayalite–magnetite buffer.

Fluid inclusions in quartz from hydrothermal veins are secondary in nature and are found in trails along healed microcracks or in clusters. Two types of fluid inclusion have been

recognized, mixed aqueous–non-aqueous volatile fluid inclusions subdivided into aqueous-rich mixed and non-aqueous volatile-rich mixed fluid inclusions, and pure aqueous fluid inclusions. The non-aqueous volatile-rich mixed fluid inclusions are one-, two-, or three-phase inclusions, whereas the aqueous-rich mixed fluid inclusions are exclusively three-phase inclusions. Both have similar low to moderate salinities (1 to 10 equiv. wt. %). The total homogenization temperatures of the aqueous-rich mixed fluid inclusions are slightly lower than those of the non-aqueous volatile-rich mixed fluid inclusions, ranging from 150 to 250 °C and 170 to 300 °C, respectively. They contain nearly pure CO<sub>2</sub>, or CO<sub>2</sub> with addition of 4.1–13.5 mole % CH<sub>4</sub> as volatile constituents. Pure aqueous fluid inclusions are two-phase with lower total homogenization temperatures (130–150 °C) and salinities ranging from 3 to 8 equiv. wt. %. They display mixing salt system characteristics, having NaCl as the dominant salt and considerable amounts of other divalent cations. Aqueous-rich mixed fluid inclusions and pure aqueous fluid inclusions exhibit a low geothermal gradient value of 18 °C/km, whereas the non-aqueous volatiles-rich mixed fluid inclusions have a high density which correspond to high geothermal gradient of 68 °C/km.

The studied granitoids are intermediate to felsic in compositions (56.9–74.6 wt. % SiO<sub>2</sub>) and have high contents of alkalis K<sub>2</sub>O (1.73–7.32 wt. %) and Na<sub>2</sub>O (1.25–5.13 wt. %) but low abundances in MnO (0.01–0.20 wt. %), MgO (0.10–3.97 wt. %), CaO (0.37–4.85 wt. %), P<sub>2</sub>O<sub>5</sub> (up to 0.90 wt. %). They display variable contents in TiO<sub>2</sub> (0.07–0.91 wt. %), Fe<sub>2</sub>O<sub>3</sub>\* (total Fe = 0.96–7.79 wt. %) and Al<sub>2</sub>O<sub>3</sub> (12.0–17.6 wt. %) contents. The granitoids show a wide range of high-field-strength elements (HFSE) and large ion lithophile elements (LILE) contents, with felsic granitoids being enriched in HFSE and the intermediate granitoids displaying in contrast high LILE concentrations. They exhibit chemical characteristics of non-alkaline to mid-alkaline, alkali-calcic, calc-alkaline, K-rich to shoshonitic, ferri-ferrous affinities. Chondrite-normalized rare earth element (REE) patterns are characterized by a strong enrichment in light compared to heavy REEs [(La/Sm)<sub>N</sub> = 3.23–9.65 and (Ga/Lu)<sub>N</sub> = 1.45–5.54, respectively], with small to significant negative Eu anomalies (Eu/Eu\* = 0.28–1.08). Ocean ridge granites (ORG) normalized multi-elements spidergrams display typical collision-related granites pattern, with characteristic negative anomalies of Ba, Nb and Y, and positive anomalies in Rb, Th and Sm.

The granitoids under study are genetically I-type granitoids (biotite granitoid, deformed biotite granitoid and mega feldspar granitoid) and one S-type granitoid (two-mica granitoid). The I-type granitoids are metaluminous (ASI: 0.70–1.00) or moderately peraluminous if highly fractionated (ASI: 1.01–1.06). The geochemistry and petrological features of these I-type granitoids argue for close genetic relationships and it is suggest that they originated from a single parent magma. The observed variability in mineralogy and major and trace element compositions in these granitoids are then the reflection of the fractional crystallization that evolved separation of plagioclase, biotite, K-feldspar and accessory minerals at the level of emplacement. The two-mica S-type granitoid is exclusively peraluminous (ASI: 1.07–1.25) and classified as a peraluminous leucocratic granitoid or leucogranite. It is marked in its CIPW normative composition by the permanent presence of corundum, ranging between 0.12 and 3.03.

The Bafoussam granitoids were emplaced in a syn- to post-collisional tectonic environment. The observed deformational features and the concentrations in Y, less than 40 ppm, confirm that they are related to an orogenesis. Whole-rock Rb–Sr isochrons defines an igneous crystallization ages of 540 ± 27 Ma for the biotite granitoid and 587 ± 41 Ma for the mega feldspar granitoid. These ages fit with the range of Pan-African granitoid ages (650–530 Ma) in West Cameroon and correspond to the Pan-African D<sub>2</sub> deformation event in the Neoproterozoic Cameroon orogenic belt. The two-mica granitoid yields an older Rb–Sr isochron age of 663 ± 62 Ma which is considered to be probably a mixing age.



The Nd–Sr isotopic compositions indicate that the I-type granitoids have been produced by partial melting of a tonalite–granodiorite source in the lower crust. This is supported by their initial  $^{87}\text{Sr}/^{86}\text{Sr}_{(600\text{ Ma})}$  ratios (0.705–0.709) and by their  $\epsilon_{\text{Nd}}(600\text{ Ma})$  values (0.2 to –6.3, mainly < 0). The two-mica granitoid was generated by partial melting of a greywacke-dominated source involving biotite-limited, biotite dehydration melting. Chemical data of the two-mica granitoid that support this hypothesis are low CaO/Na<sub>2</sub>O (0.11–0.38) and Sr/Ba (0.20–0.30), the high Rb/Sr (2.26–7.00), the high initial  $^{87}\text{Sr}/^{86}\text{Sr}_{(600\text{ Ma})}$  ratios ranging from 0.708 to 0.720, the large range in Al<sub>2</sub>O<sub>3</sub>/TiO<sub>2</sub> (47–204) and the negative  $\epsilon_{\text{Nd}}(600\text{ Ma})$  values (–9.9 to –14.0). Moreover, the higher initial  $^{87}\text{Sr}/^{86}\text{Sr}_{(600\text{ Ma})}$  ratios of the two-mica granitoid are consistent with an upper crust origin. The depleted mantle Nd model ages ( $T_{\text{DM}}$ ) of 1.3–2.3 Ga indicate that the studied granitoids originated by partial melting of Paleoproterozoic and Mesoproterozoic crust, with limited mantle-derived magma contribution. The high initial  $^{87}\text{Sr}/^{86}\text{Sr}_{(600\text{ Ma})}$  ratios of these granitoids coupled with the wide negative  $\epsilon_{\text{Nd}}(600\text{ Ma})$  values strongly suggest a very long residence time in the crust of their protoliths before the melting event.

The petrologic signatures of the Bafoussam granitoids are similar to those described in other Pan-African belts of western Gondwanaland such as the neighbouring provinces of Nigeria and the Central African Republic, as well as in the Borborema Province of northeastern Brazil. This supports the previous hypothesis that the Central African fold Belt including Cameroon, Nigeria and the Central African Republic provinces has a continuation in Brazil.

## ZUSAMMENFASSUNG

Die Region Bafoussam im westlichen Kamerun ist Teil des "Cameroon Neoproterozoic orogenic belt" (nördlich des Kongo Kratons), welcher zum "Central African Fold Belt" (CAFB) gehört. Die Entstehung des CAFB hängt ursächlich mit der Kollision zwischen dem konvergierenden Westafrikanischen Kraton, dem Sao Francisco – Kongo Kraton und dem Sahara Megakraton zusammen. Die untersuchten Gesteine, im wesentlichen Granitoide, die während der pan-afrikanischen Orogenese in Migmatite und Gneisse intrudierten, sind auf einer Fläche von ca. 1000 km<sup>2</sup> aufgeschlossen. Die Platznahme der Bafoussam Granitoide wurde zum einen durch die N 30 °E verlaufende transversale Störungszone entlang der Verlängerung der "Cameroon Volcanic Line" beeinflusst, zum anderen durch die N 70 °E verlaufende "Central Cameroon Shear Zone". Im Gelände finden diese beiden Richtungen Ausdruck in der Schieferung und Foliation der Gesteine, der Orientierung von Störungen, sowie der Anordnung von vulkanischen Kegeln.

Das untersuchte Gebiet in der Umgebung von Bafoussam beherbergt vier Typen von Granitoiden: (i) Biotit-Granitoid, (ii) deformierter Biotit-Granitoid, (iii) Mega-Feldspat-Granitoid und (iv) Zwei-Glimmer-Granitoid. Generell sind die Granitoide als ausgelängte Plutone mit eingeschlossenen Enklaven von Mafiten (amphibolführende, biotitreiche und metagabbroide Typen) aufgeschlossen und werden teilweise von jüngeren Quarz-, Pegmatit- und Aplitdykes durchzogen. Petrographisch reichen die Granitoide von dominierendem Syenogranit über Alkali-Feldspat-Granit, Granodiorit, Monzogranit, Quarz-Syenit, Quarz-Monzonit bis zu Quarz-Monzodiorit. Hauptgemengteile sind Kalifeldspat, Quarz, Plagioklas und Biotit, die zusammen mit teilweise vorhandenem Amphibol und Akzessorien wie Apatit, Zirkon, Monazit, Titanit, Allanit, Ilmenit und Magnetit auftreten. Serizit, Epidot und Chlorit sind Sekundärminerale. Der Zwei-Glimmer-Granitoid enthält zusätzlich primären Muskovit und gelegentlich magmatischen Granat.

Die Granitoide enthalten als Kalifeldspat generell Orthoklas (Mikroklin und Orthoklas: Or<sub>81-97</sub>Ab<sub>19-3</sub>), Plagioklas ist hauptsächlich Oligoklas mit etwas Albit und Andesin (An<sub>3-35</sub>Ab<sub>96-64</sub>). Biotit ist Fe-reich (Merxene und Lepidomelan mit etwas Siderophyllit) mit hohen Fe<sup>2+</sup>/(Fe<sup>2+</sup> + Mg) Verhältnissen zwischen 0.40–0.80. Es handelt sich um reequilbrierten primären Biotit, der ein kalk-alkalines, peraluminöses Ausgangsgestein für die Granitoide anzeigt. Amphibol ist edenitische und magesium-hastingsitische Hornblende mit hohem Mg/(Mg + Fe<sup>2+</sup>) Verhältnis von 0.50–0.62. Die Entstehung der Hornblende wurde durch edenitische, tschermakitische, pargasitische und hastingsitische Substitutionen bestimmt. Primärer Muskovit ist eisenreich [Fe<sup>2+</sup>/(Fe<sup>2+</sup> + Mg) = 0.52–0.82] und hat Celadonit- und Paragonit-Substitutionen erfahren. Granat ist Almandin-Spessartin (X<sub>Fe</sub> = 0.99 und X<sub>Mn</sub> = 0.46–0.56). Die idiomorphe Ausbildung des Granats und das Fehlen von Einschlüssen in Kombination mit hohen Mn und Fe<sup>2+</sup> Gehalten (2.609–3.317 a.p.f.u und 2.646–3.277 a.p.f.u) und niedrigen Mg-Gehalten (0.012–0.038 a.p.f.u) liefern deutliche Hinweise für den plutonischen Ursprung des Granats. Für die Sprossung des Granats wird das Mn-Verarmungsmodell angenommen; danach wächst initialer Granat, was eine frühe Mn-Verarmung der Schmelze zur Folge hat.

Aluminium-in-Hornblende- und Phengit-barometrische Abschätzungen zeigen, dass die Granitoide bei 4.2 ± 1.1 bis 6.6 ± 1.0 kbar kristallisierten, was einer Platznahmetiefe von 15–24 km entspricht. Temperaturbestimmungen über die Zirkon- und Apatit-Sättigung und Hornblende-Plagioklas Thermometrie ergeben Platznahmetemperaturen von 772 ± 41 bis 808 ± 34 °C. Mit Ausnahme des Zwei-Glimmer-Granitoids liefert die Paragenese Titanit-Magnetit-Quarz eine Sauerstoff-Fugazität zw. 10<sup>-17</sup> und 10<sup>-13</sup>, was darauf schliessen lässt, dass die Granitoide einem oxidierten Magma entstammen. Da dem Zwei-Glimmer-Granitoid Magnetit

fehlt, entstand er aus einem Magma unter reduzierenden Bedingungen unterhalb des Quarz-Fayalit-Magnetit Puffers.

Fluideinschlüsse in Quarz aus hydrothermalen Gängen sind sekundärer Natur und als Spuren entlang verheilter Mikrorisse oder als Cluster zu finden. Zwei Sorten von Fluideinschlüssen wurden unterschieden, gemischte wässrige-nicht-wässrige volatile Fluideinschlüsse, die wiederum in wässrige gemischte und nicht-wässrige volatilreiche gemischte Fluideinschlüsse unterteilt werden und zweitens rein wässrige Einschlüsse. Die nicht-wässrigen volatilreichen gemischten Fluideinschlüsse sind ein-, zwei-, oder drei-phasige Einschlüsse. Beide Sorten besitzen ähnlich niedrige bis mittlere Salinitäten (1 bis 10 equiv. wt. %). Die Homogenisierungstemperatur der wässrigen gemischten Fluideinschlüsse ist geringfügig niedriger als die der nicht-wässrigen volatilreichen, mit Werten zw. 150 bis 250 °C bzw. 170 bis 300 °C. Sie enthalten nahezu reines CO<sub>2</sub>, oder CO<sub>2</sub> mit 4.1–13.5 mol % CH<sub>4</sub> als flüchtigen Bestandteil. Reine wässrige Fluideinschlüsse sind zwei-phasig mit niedrigerer Homogenisierungstemperatur (130–150 °C) und Salinitäten zw. 3 und 8 equiv. wt. %. Sie zeigen Salzmischungscharakteristika mit NaCl als dominantem Salz sowie gewissen Mengen an anderen divalenten Kationen. Wässrige gemischte Fluideinschlüsse und reine wässrige Einschlüsse zeigen einen niedrigen geothermalen Gradienten von 18 °C/km, wohingegen nicht-wässrige gemischte Fluideinschlüsse eine hohe Dichte aufweisen, was einem hohen geothermalen Gradienten von 68 °C/km entspricht.

Die untersuchten Granitoide besitzen eine intermediäre bis saure Zusammensetzung (56.9–74.6 wt. % SiO<sub>2</sub>) und zeigen hohe Alkali-Gehalte (K<sub>2</sub>O = 1.73–7.32 wt. %, Na<sub>2</sub>O = 1.25–5.13 wt. %), aber niedrige Gehalte an MnO (0.01–0.20 wt. %), MgO (0.10–3.97 wt. %), CaO (0.37–4.85 wt. %) und P<sub>2</sub>O<sub>5</sub> (bis zu 0.90 wt. %), zudem besitzen sie variable Gehalte an TiO<sub>2</sub> (0.07–0.91 wt. %), Fe<sub>2</sub>O<sub>3</sub>\* (total Fe = 0.96–7.79 wt. %) und Al<sub>2</sub>O<sub>3</sub> (12.0–17.6 wt. %). Die Granitoide zeigen ein weites Spektrum bezogen auf ihren Gehalt an high-field-strength elements (HFSE) und large-ion-lithophile elements (LILE), wobei saure Granitoide an HFSE angereichert sind und intermediäre Granitoide hohe Konzentrationen von LILE aufweisen. Die Granitoide zeigen chemische Signaturen nicht-alkaliner bis mittel-alkaliner, alkali-kalziumreicher, kalkalkaliner, K-reicher bis shoshonitischer und eisenreicher Magmatite. Chondrit-normalisierte Seltene Erden Element (SEE)-Verteilungsmuster sind durch eine starke Anreicherung der leichten SEE [(La/Sm)<sub>N</sub> = 3.23–9.65] verglichen mit schweren SEE [(Ga/Lu)<sub>N</sub> = 1.45–5.54] gekennzeichnet sowie durch geringe bis signifikante negative Eu Anomalien (Eu/Eu\* = 0.28–1.08). Auf die Zusammensetzung von Ocean Ridge Granit (ORG) normalisierte Multielement-Spiderdiagramme zeigen Verteilungsmuster, die typisch sind für Granite aus Kollisionsorogenen, mit charakteristischen negativen Anomalien von Ba, Nb und Y sowie positiven Anomalien von Rb, Th, Sm.

Die untersuchten Granitoide sind genetisch I-Typ Granitoide (Biotit-Granitoid, deformierter Granitoid und Mega-Feldspat-Granitoid) mit einem S-Typ Granitoid (Zwei-Glimmer-Granitoid). Die I-Typ Granitoide sind metaluminös (ASI: 0.70–1.00) oder schwach peraluminös bei starker Fraktionierung (ASI: 1.01–1.06). Die geochemischen und petrologischen Merkmale dieser I-Typ Granitoide sprechen für eine enge genetische Verwandtschaft der Gesteine untereinander und lassen somit eine einzige Quelle als Ausgangsmagma vermuten. Die beobachteten Unterschiede in der Mineralogie und in Haupt- und Spurenelementzusammensetzung spiegeln somit die fraktionierte Kristallisation wieder, welche für die Trennung von Plagioklas, Biotit, K-Feldspat und Akzessorien während der Platznahme verantwortlich ist. Der S-Typ Zwei-Glimmer-Granitoid ist ausschliesslich peraluminös (ASI: 1.07–1.25) und wird als peraluminöser leukokrater Granitoid oder Leukogranit klassifiziert. In

der normativen CIPW Zusammensetzung ist er durch die durchgehende Präsenz von Korund gekennzeichnet, mit Werten zw. 0.12 und 3.03.

Die Platznahme der Bafoussam Granitoide fand in einem tektonischen syn- bis post-Kollisions-Umfeld statt. Die beobachteten Deformationsmerkmale und die Konzentration an Y mit Werten meist unter 40 ppm bestätigen, dass die Granitoide mit einer Orogenese verbunden sind. Rb–Sr Gesamtgesteins-Isochronen ergeben ein Kristallisationsalter von  $540 \pm 27$  Ma für den Biotit-Granitoid und  $587 \pm 41$  Ma für den Mega-Feldspat-Granitoid. Diese Alter entsprechen denen anderer pan-afrikanischer Granitoide (650–530 Ma) in West-Kamerun und stimmen mit dem pan-afrikanischen  $D_2$  Deformationereignis im "Cameroon Neoproterozoic Orogenic Belt" überein. Der Zwei-Glimmer Granitoid liefert ein Rb–Sr Isochronenalter von  $663 \pm 62$  Ma, was wahrscheinlich als Mischungsalter zu deuten ist.

Die Zusammensetzung der Nd–Sr Isotope zeigt an, dass die I-Typ Granitoide durch partielles Schmelzen einer tonalitisches-granodioritischen Quelle entstanden sind. Dies wird gestützt durch ihr initiales  $^{87}\text{Sr}/^{86}\text{Sr}$  Verhältnis (0.705–0.709) sowie durch ihre  $\epsilon\text{Nd}_{(600 \text{ Ma})}$  Werte (0.2 bis –6.3, meist <0). Der Zwei-Glimmer-Granitoid entstand durch partielles Aufschmelzen einer Grauwacken-dominierten Quelle mit Biotit-Entwässerungs-Schmelzen. Chemische Daten des Zwei-Glimmer-Granitoids, die diese Hypothese bestätigen, sind niedrige CaO/Na<sub>2</sub>O (0.11–0.38) und Sr/Ba (0.20–0.30) Gehalte, hohe Rb/Sr (2.26–7.00) Gehalte, sowie die grosse Spanne im Al<sub>2</sub>O<sub>3</sub>/TiO<sub>2</sub> Verhältnis (47–204) und negative  $\epsilon\text{Nd}_{(600 \text{ Ma})}$  Werte (–9.9 bis –14.0). Desweiteren sprechen die höheren initialen  $^{87}\text{Sr}/^{86}\text{Sr}_{(600 \text{ Ma})}$  Verhältnisse des Zwei-Glimmer-Granitoids für einen Ursprung aus der oberen Kruste. Die Nd-Modellalter eines verarmten Mantels ( $T_{\text{DM}}$ ) von 1.3–2.3 Ga geben Hinweise auf die Entstehung der untersuchten Granitoide durch partielles Aufschmelzen paläozoischer und mesoproterozoischer Kruste, mit eingeschränkter Zufuhr von Mantelmagma. Die hohen initialen  $^{87}\text{Sr}/^{86}\text{Sr}_{(600 \text{ Ma})}$  Werte der Granitoide, verbunden mit negativen  $\epsilon\text{Nd}_{(600 \text{ Ma})}$  Werten sprechen stark dafür, dass der Protolith dieser Granitoide eine sehr lange Zeit in der Kruste verbrachte, bevor es zum Schmelzereignis kam.

Die petrologischen Signaturen der Bafoussam Granitoide ähneln denen von bereits beschriebenen Granitoiden des pan-afrikanischen Gürtels in West-Gondwana, z. B. aus den angrenzenden Provinzen von Nigeria und der Zentral Afrikanischen Republik sowie der Borborema Provinz im nordöstlichen Brasilien. Dies unterstützt die Hypothese, dass der "Central African Fold Belt" von Kamerun, Nigeria und der Zentral Afrikanischen Provinz seine Fortsetzung in Brasilien findet.

## ACKNOWLEDGEMENTS

I am extremely grateful to my supervisor Dr. habil. U. Schüssler for his invaluable support, encouraging comments, constructive suggestions and critical review of the different chapters. His advice and assistance during the electron microprobe analysis is highly appreciated. Special thanks are due to Professor Dr. B. Schulz (University of Erlangen) for his enthusiasm for discussions, challenging and critical comments on various sections of the thesis.

Many thanks are extended to Dr. J.-P. Tchouankoué (University of Yaoundé I, Cameroon) who initiated this project. His willingness for assistance during the field work is highly appreciated. Dr. habil. E. Njonfang and Dr. T. Njanko are thanked for the great instructive time in the field. I appreciate the companionship of my brother, D.C. Kamdoun-Fonkwe during fieldwork.

Professor Dr. R. Klemm, Mrs R. Baur and Dr. H. Brätz are acknowledged for their support in the XRF- and the LA-ICPMS- analyses, Mr. P. Späthe for the preparation of thin and double polished sections of the rocks, Mr. K.-P. Kelber for the introduction to digital photography and Mrs. A. Kirchner for the administrative assistance. I wish to express my gratitude to Dr. C. Nzolang for carrying out the Rb–Sr and Sm–Nd whole-rock isotope measurements at the Graduate School of Science and Education, Niigata University (Japan).

My sincere gratitude goes to Dr. T. Graupner for the valuable assistance during the microthermometric measurements. His useful comments and discussions concerning the fluid inclusion chapter are greatly appreciated. I am indebted to Professor Dr. H. E. Frimmel for providing me with a computer program used in the density determination, the stimulating discussions and the critical comments on the fluid inclusion section.

I am thankful to Dr. habil. A. Zeh for his willing assistance, providing computer softwares, as well as guidance on their use to process analytical data. Dr. K. Drüppel, Dr. S. Brandt and Dipl.-Min. L. J. Millonig are acknowledged for their assistance and a good working atmosphere. The continuous support of Dr. A. A. Ganwa is highly appreciated.

My special thanks are addressed to my family for their encouragement and support during my work. Dr. B. Takam-Mangoua is appreciated for his advice and Dr. J. Mutanyatta-Comar for her friendship, being there for me when I needed to talk to someone especially during the challenging times of my work and her patience in improving my English language that has greatly contributed to the achievement of this study. Diane Guemfouo-Yoota is acknowledged for her great and encouraging support. Many thanks to all my friends.

Last, but not least, I am very grateful to the German Academic Exchange Service (Deutscher Akademischer Austausch Dienst, DAAD) for financial support without whom this work would not have been possible.

## 1 INTRODUCTION

### 1.1 Geological setting of Cameroon

The Bafoussam area is situated in the West province of Cameroon, 300 km north-west of the capital Yaoundé. The west province is bordered by Adamaoua and the north-west provinces to the North, the south-west province to the West, the Littoral province to the South and the Centre province to the East (Fig. 1.1).

An outline of the geological setting of Cameroon is given for a better assessment of the geology of the studied area in the Cameroon context. In the following, the four structural domains in Cameroon including the Congo craton, the Neoproterozoic orogenic belt, the sedimentary basins and the Cameroon Volcanic Line are described.

#### 1.1.1 Congo craton

The Congo craton occupies a large part of the Southern Central Africa. It extends into the Central Africa Republic to the East and into the Republics of Equatorial Guinea, Gabon, Congo, Congo Democratic and Tanzania to the South (Bessoles and Trompette, 1980). Its northern margin, well-preserved in the south of Cameroon (Fig. 1.2), is called the *Ntem complex* (Bessoles and Lasserre, 1977).

The northern border of the Congo craton has been widely discussed, but until now is still not clearly defined. It differs when considering the geophysical (Dorbath et al., 1985; Dumont, 1986; Toteu et al., 2004) or geological and lithological–structural (Bessoles and Trompette, 1980; Cornacchia and Dars, 1983) points of view (see Fig. 1.4). The geophysical margin of the Congo craton, along which most of the seismic activities of south Cameroon have been documented (Ateba et al., 1992), lies north of its geological border. The latter is marked by a major thrust at the contact with the Neoproterozoic (Pan-African) orogenic belt represented by the Yaoundé schist belt.



Figure 1.1: Geographical overview map of Cameroon. The studied area is marked by a filled square.



The Ntem complex is composed predominantly of Archean basement that suffered slight Eburnean or Trans-Amazonian reactivation at  $2.0 \pm 0.2$  Ga ago and is discordantly overlain by Proterozoic sedimentary covers that constitute the Yokadouma and Dja series (Bessoles and Lasserre, 1977; Alvarez, 1995). During the Pan-African orogeny, the Ntem complex was overthrust towards the SW by the Neoproterozoic orogenic belt (see Fig. 1.2: Nzenti et al., 1988).

An association of several lithological groups is distinguished within the Ntem complex:

- **The greenstone belt suites** consist of banded siliceous and ferrogineous metasediments (Banded iron formation, BIF), aluminous metasediments and mafic to ultramafic rocks. Actually, they are only found as xenoliths within the intrusive rocks and indicate an older age for their formation (Nsifa and Riou, 1990). The metabasites and the metasediments from the greenstone belt suites yielded an age of  $3147 \pm 2.9$  Ma through the Pb–Pb evaporation methods on zircons, and Sm–Nd model ages range from 3.1–3.6 Ga, respectively (Toteu et al., 1994; Tchameni, 1997; Shang, 2001).

- **The intrusive rocks** are composed of charnockitic granitoids and non-charnockitic rocks comprising tonalite and high-K granitoids:

The charnockitic granitoids and the tonalite show the tonalite–trondhjemite–granodiorite (TTG) affinities (Nédélec et al., 1990). The charnockites have a Mesoarchean age of emplacement, between 2.8 and 2.9 Ga, as indicated by U–Pb on zircons as well as Rb–Sr, Sm–Nd whole-rock isochrons and zircon  $^{207}\text{Pb}/^{206}\text{Pb}$  evaporation data (Delhal and Ledent, 1975; Cahen et al., 1984; Tchameni, 1997; Shang et al., 2004a, b). These ages have been regarded as the charnockitization age (Cahen et al., 1984; Toteu et al., 1994b; Tchameni, 1997). In comparison with the charnockitic granitoids, the tonalite suite yields a crystallization age of ca. 2.8 Ga that was reported from Rb–Sr isochron and Pb–Pb zircon evaporation data (Lasserre and Soba, 1976a; Shang, 2001). The rocks from the greenstone belt formations and the TTG suites underwent several degrees of partial melting that led to the genesis of banded formations (Maurizot et al., 1986; Nsifa and Riou, 1990; Nédélec et al., 1993) and high-K granitoids (Nédélec et al., 1990; Tchameni et al., 2000).

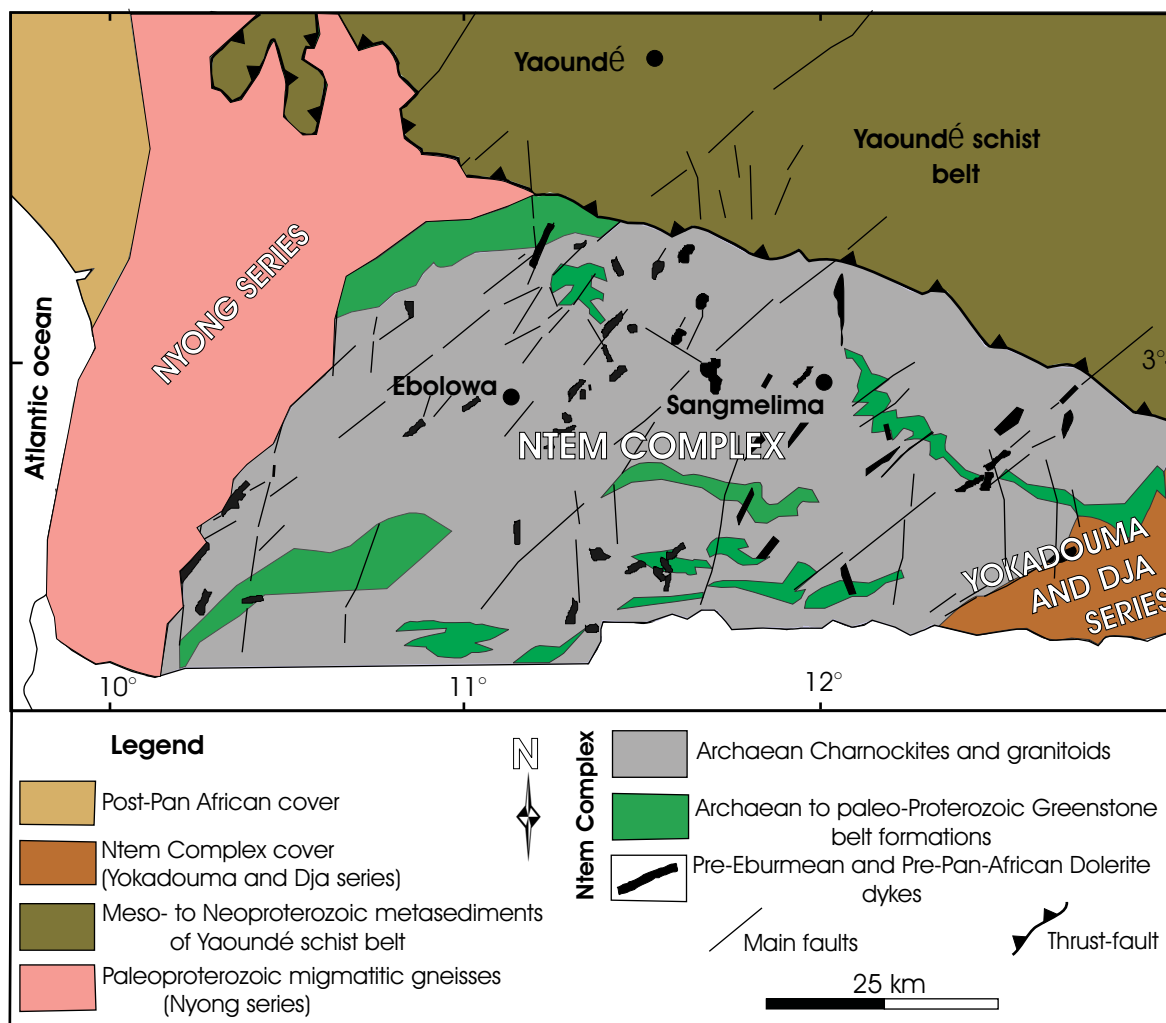


**Figure 1.2:** General geologic map of South Cameroon showing the different geologic formations of the Ntem complex, northern margin of the Congo craton, and the thrust contact with the Neoproterozoic (Pan-African) orogenic belt (adapted from Maurizot et al., 1986 and Penaye et al., 2004). The studied area, Bafoussam, is located further to the North and does not appear in this map.

The high-K granitoids comprise of calc-alkaline granodiorites, granites and leucogranites that occur as intrusions of late to post-orogenic origin in the older TTG suites and greenstone belts (Kornprobst et al., 1976; Nédélec et al., 1990; Tchameni, 1997). Tchameni et al. (2000) obtained a Pb–Pb zircon age of 2.6 Ga for the K-rich granitoid intrusions which end the Archean time in the Ntem complex.

- **The banded formation** predominates within the Nyong unit, while it is scattered in the Ntem unit. It is composed of various migmatitic gneisses including leptinites, biotite gneisses, amphibole ± biotite gneisses and charnockitic gneisses, which are mostly orthoderived, and of quartzites associated with pyroxene-garnet-bearing amphibolites. Following Toteu et al. (1994) and Tchameni (1997), the banded formation rocks were strongly reactivated during Eburmean

magmatic event (~ 2050 Ma) and range in age between 2.0 and 2.9 Ga, obtained by U–Pb analyses on zircons.

- The late- to post-tectonic *alkaline syenites* cross-cut the members of the TTG suites and the greenstone belt suites (Kornprobst et al., 1976). They intruded probably during early Proterozoic times around 2.3 Ga, as suggested by Pb–Pb zircon evaporation ages, and are derived from the pre-existing continental crust (Tchameni et al., 2001).

- *The metadolerites* are distinguished in two generations, the first prior to the Eburnean orogeny is dated at 2.1 Ga and the second, prior to the Pan-African orogeny seems to have been emplaced around 1.0 Ga ago (Vicat et al., 1996; Tchameni, 1997). These structurally youngest rocks are tholeiitic in composition and occur as lens-shaped elongated dykes, exposed in the older formations presented above. The metadoleritic dykes represent the final magmatic activity in the Ntem complex.

From a structural point of view, the Congo Craton was affected by three major periods of deformation along its northwestern margin (Tchameni, 1997; Shang, 2001):

(1) The first deformation period by roughly coaxial strains in the entire complex can be correlated with the successive diapiric emplacement of the granitoids into the greenstone belts contemporaneous to granulite facies metamorphism dated at  $2055 \pm 5$  Ma (Toteu et al., 1994b; Lerouge et al., 2004). Generally, it is characterized by a foliation, vertical stretching along a vertical lineation and isoclinal folds observed in the relict greenstone belts and the TTG series.

(2) The second period of deformation, synchronous with an amphibolite facies metamorphism, is marked by the development of a sinistral shear-plane oriented north-south to N 50 °E, and partial melting of the TTG suites and their country rocks. The syenites intruded during this second tectonic episode.

(3) The third deformation period is related to the overtrusting Pan-African schistose formations, a multitude of C<sub>3</sub> structures (mylonitic and shear corridor) of the Pan-African origin are observed in TTG rocks along the thrusting front.

Equivalent lithological formations with similar ages have been reported in the other parts of Congo Craton in neighbouring countries to the South as Equatorial Guinea, Gabon and Congo (Cahen et al., 1984; Feybesse et al., 1998) as well as in the northeastern part of the São Francisco Craton in Brazil (Alkmin et al., 2001; Engler et al., 2002). These results support the model that

the Congo and the São Francisco cratons were linked during the Eburnean–Trans-Amazonian orogeny around 2050 Ma ago (Ledru et al., 1994). These cratons are delimited by orogenic belts mostly of Neoproterozoic (Pan-African) age (Cahen et al., 1984).

### 1.1.2. Neoproterozoic orogenic belt

The orogenic belt of Neoproterozoic age north of the Congo craton represents the most conspicuous feature of the Precambrian of Cameroon and covers the complete remaining area of the country. This part of Cameroon was subjected to the Pan-African event (Lasserre and Soba, 1976b; Bessoles and Lasserre, 1977).

The term *Pan-African* was originally defined by Kennedy (1964) as a thermo-tectonic event that happened at about 500 Ma, affecting large areas surrounding the African cratons. It is now referred to as summarizing orogenic events in the latest Proterozoic to earlier Paleozoic, ~ 700–500 Ma (Jackson and Ramsay, 1980; Mallard and Rogers, 1997; Black and Liegeois, 1993). It is thus mostly used as a general designation for the late Neoproterozoic collisional events between the component cratons of West Gondwana and the deformational events along the East Gondwana paleo-pacific margin. Besides Africa and the Arabian-Nubian Shield, the usage of Pan-African is extended to the other former Gondwanaland continents (recognized as *Pan-Gondwanaland*) of South America (here known as *Brasiliano*), India, Antarctica (here referred to as *the Ross Orogen*), Australia (here termed *Delamerian*) (Trompette, 1994; Yoshida and Santosh, 1995; Veevers, 2003; 2004; Camacho et al., 2002) and also to North America and Europe (O'Brien et al., 1983; Rogers et al., 1995).

Clifford (1970) distinguished two distinct types of Pan-African fold belts in Africa: (1) *Geosynclinal fold belts* consisting of important metasedimentary and metavolcanic rocks deposited or emplaced during the period between ~ 1200 and ~ 550 Ma (e.g., The Arabian-Nubian Shield, the Damara fold belt of southern Africa and the Trans-Saharan fold belt of west Africa); and (2) *Vestigial fold belts* formed mainly by rejuvenated Archean or Early Mesoproterozoic rocks with or without intrusions of Pan-African plutons (e.g., Mozambique fold belt, parts of the west Sudanese and the southern Ethiopian sector of the Arabian-Nubian Shield, Nigeria and northern Cameroon).

The Neoproterozoic orogenic belt of Cameroon belongs to the E-trending Oubanguides orogenic belt (Pin and Poidevin, 1987) also variably termed the Pan-African North-Equatorial Fold Belt (Nzenti et al., 1988) or also used in the present work, the Central African Fold Belt (Trompette, 1994: 1997). The Central African Fold Belt continues to the west to Brazil where it corresponds to the Sergipane fold belt or Sergipe (Davison et al., 1989). To the East, it extends from the northern part of the Mozambique fold belt in the south to Sudan in the north, reaching the Arabian-Nubian Shield. Bessoles and Trompette (1980) have interpreted the Central African fold belt as a Pan-African “mobile-area” between the West African and Congo Cratons, as well as a possible third craton, the Sahara Metacraton (Abdelsalam et al., 2002). The Sahara Metacraton mentions a craton that was largely remobilized during an orogenic event after 700 Ma (Black and Liégeois, 1993), but is still identifiable mainly through its rheological, geochronological and isotopic characteristics.

Prior to Atlantic rifting, the central African fold belt together with the adjacent Trans-Sahara fold belt to the Northwest and the Sergipane fold belt to the southwest in Northeast Brazil formed the northern part of the Pan-African/Brasiliano orogenic belt (Figs. 1.3A, B: Castaing et al., 1993; Trompette, 1994). This portion of the large orogen plausibly resulted from the roughly submeridional collision between the converging West African craton, the Sahara metacraton, the joined São Francisco–Congo craton, Amazonian craton and the NE Brazil – Central African Pan-African mobile domains during the amalgamation of western Gondwana at the end of the Proterozoic or Pan-African/Brasiliano orogeny (Poidevin, 1985; Castaing et al., 1993: 1994; Rogers et al., 1995; Trompette, 1994: 1997: 2000; Ferré et al., 2002; Veevers, 2003: 2004). According to Trompette (1994), the Pan-African/Brasiliano orogeny was the last important orogenic event affecting the Pan-African or Brasiliano belts.

Within the Cameroon Neoproterozoic orogenic belt, the external nappes of regional extent on the northern margin of the Congo craton, the granulitic metamorphism, intensive plutonism associated with crustal melting, regional strike-slip faults and the possible presence of molassic basins are interpreted by various workers as Pan-African collisional imprints (Pin and Poidevin, 1987; Nzenti et al., 1988; Penaye et al., 1989: 1993; Toteu et al., 1990; 2004), based mainly on the tectonic evolution and general aspects of magmatic activity. The geochronologic data

constrain the collision period in the time interval of 630–580 Ma (Toteu et al., 1994; Ferré et al., 2002; Ngako et al., 2003).

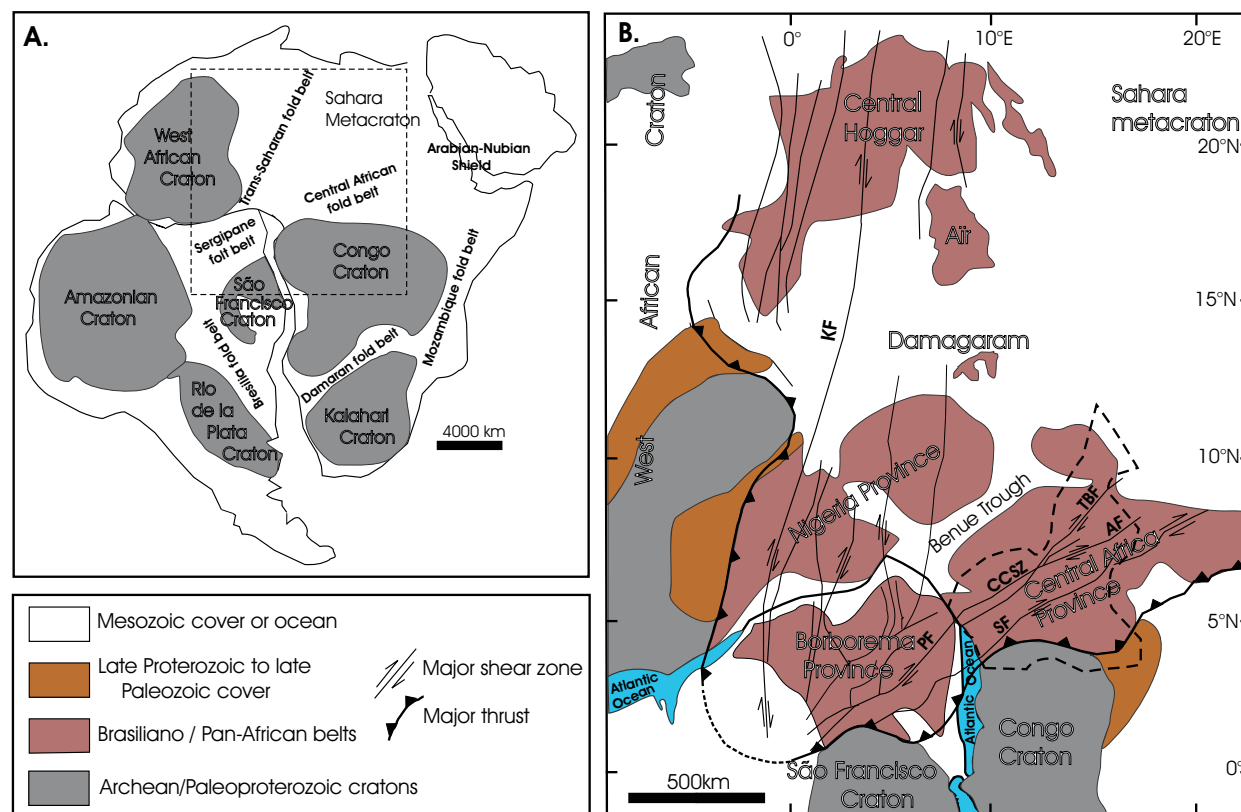


**Figure 1.3:** (A) General distribution of the Pan-African/Brasiliano cratons and major orogenic belts within Western Gondwana adapted from Trompette (2000) and Abdelsalam et al. (2002). (B) Geological sketch map of west-central Africa and northern Brazil showing the cratonic masses and the Pan-African/Brasiliano provinces in a Gondwana (pre-drift) reconstruction, modified from Castaing et al. (1993); Toteu et al. (2001) and Ferré et al. (2002). TBF: Tcholliré-Banyo Fault, AF: Adamaoua Fault, CCSZ: Central Cameroon Shear Zone, PF: Pernambuco Fault, SF: Sanaga Fault, KF: Kandi Fault. Dashed outline roughly marks the boundary of Cameroon.

Based on the previous field work as well as petrographic, structural and isotopic investigations within the Neoproterozoic orogenic belt of Cameroon, several lithostratigraphic domains can be distinguished (Bessoles and Lasserre, 1977; Soba, 1989) (Fig. 1.4).

### 1.1.2.1 Paleoproterozoic gneissic basement

The Paleoproterozoic gneissic basement in Cameroon roughly oriented NNE–SSW, have been remobilized during the Pan-African orogeny. It includes the Nyong series and the remnants cropping out further north within the Neoproterozoic orogenic belt.

The Nyong series is a NNE–SSW trending band located at the NW corner of the Congo Craton (see Figs. 1.2 and 1.4). It consists of: (1) remnants of greenstone belts, such as pyroxene meta-quartzites and garnet-rich amphibol-pyroxenites and gneisses; (2) migmatitic grey gneisses of TTG composition; and (3) syn- to late-tectonic charnockites, augen metadiorites, porphyritic granites, granodiorites and alkaline syenites; post-tectonic metadolerites (Toteu et al., 1994; Lerouge et al., 2004; Penaye et al., 2004). The Paleoproterozoic structures and mineral assemblages are well preserved in these rocks. Rb–Sr whole rock isochron age of  $2850 \pm 65$  Ma has been derived from gneisses of TTG composition (Lasserre and Soba, 1979). Toteu et al. (1994) reported U–Pb zircon age and garnet Sm–Nd age of  $2037 \pm 10$  Ma and  $\sim 2050$  Ma, respectively that indicate the formation of the Nyong series during the Paleoproterozoic, prior or synchronously with the dated 2.05 Ga metamorphism. The Nyong series is interpreted as a proximal domain characterized by reworking and recycling of the adjacent Archean cratonic crust (Penaye et al., 2004).

Within the Neoproterozoic orogenic belt, the Paleoproterozoic high-grade metamorphic rocks are observed particularly to the east of the Tcholliré-Banyo fault, around Ngaoundéré and north of Bafia, as xenoliths in the Pan-African granitoids. The most common rock types include: (1) a metasedimentary or volcanosedimentary sequence including hornblende–biotite and biotite–garnet gneisses, meta-arkoses and metaquartzites which are frequently associated with iron formations, scattered bands of garnet–pyroxene amphibolite, garnetiferous and calc-silicate rocks; and (2) metaplutonics of dominant dioritic and granodioritic composition (Penaye et al., 1989; Ganwa, 1998). In contrast to the Nyong series, the Paleoproterozoic structures here have been deeply reworked during the Pan-African orogeny (Toteu et al., 2001). Metamorphic studies carried out by Penaye (1988) in northern Cameroon (Buffle Noir and Mbé areas, and South-East of Poli) indicate the presence of only relict granulitic assemblages preserved in both para- and orthogneisses which must predate the climax of the Pan- African deformation ( $D_1$ ) and an

associated migmatization. Furthermore, Penaye et al. (1989) and Toteu et al. (1990) reported U–Pb intercept ages of  $2130 \pm 20$  Ma and  $588 \pm 50$  Ma for granet–pyroxene amphibolite and  $2104 \pm 7$  Ma and  $580 \pm 11$  Ma for hornblende–biotite gneisses from Buffle Noir and Mbé areas, respectively. To the south-west on the other hand, the migmatitic biotite gneiss from Yabassi and hornblende–biotite gneisses from Makénéne in the Bafia region (Toteu et al., 2001) yield U–Pb upper intercept ages of  $\sim 2175$  Ma and  $2018 \pm 9$  Ma, and lower intercept ages of  $\sim 600$  Ma and  $692 \pm 113$  Ma, respectively. The Sm–Nd signatures and  $T_{DM}$  ages (2.2–3.0 Ga) indicate that these Paleoproterozoic rocks were derived from recycled Paleoproterozoic (Birimian) crust (Ganwa, 1998; Toteu et al., 2001).

### 1.1.2.2 Late Mesoproterozoic to Neoproterozoic schist belts

Three major schist belts are recognized, namely the Poli, Lom and Yaoundé schist belts representing the volcano-sedimentary basins. The schist belts were first interpreted as low-grade metamorphic units of Mesoproterozoic age (Bessoles and Trompette, 1980). However, more recent investigations showed that the schist belts also contain some high-grade metamorphic rocks, including granulites, which were previously attributed to an older basement complex (Nédélec et al., 1986; Toteu et al., 1994).

- **The Poli schist belt** (Angoua, 1988; Njel, 1988; Ngako et al., 1989) is comprised of metasediments having argillite- and greywacke-type compositions, and layers of tholeiitic to alkaline metavolcanic units (basalts and rhyolites). Toteu et al. (1990) reported an age of  $830 \pm 11$  Ma (U–Pb on zircons) for metarhyolites. The Poli schist belt indicates a retrogressive metamorphism of Pan-African age ( $T = 650$  °C and  $P = 5–7$  kbar; Nzenti et al., 1992). Copper mineralization has been noticed within this volcano-sedimentary basin (Le Fur, 1971).

- **The Lom schist belt** includes micaschists, quartzites in places associated with conglomerates, metasediments and acidic metavolcaniclastic rocks displaying a Pan-African amphibolite facies metamorphism. The schists of volcano-sedimentary origin yield a discordia with a lower intercept of  $709 \pm 19$  Ma and an imprecise upper intercept of  $2472 \pm 104$  Ma (U–Pb zircon age; Soba et al., 1991).

- **The Yaoundé schist belt** (Penaye et al., 1993; Ngnotué et al., 2000; Nvondo et al., 2003) marks the southern limit of the Neoproterozoic belt and thrusts onto the Congo craton (Figs. 1.3–1.5).



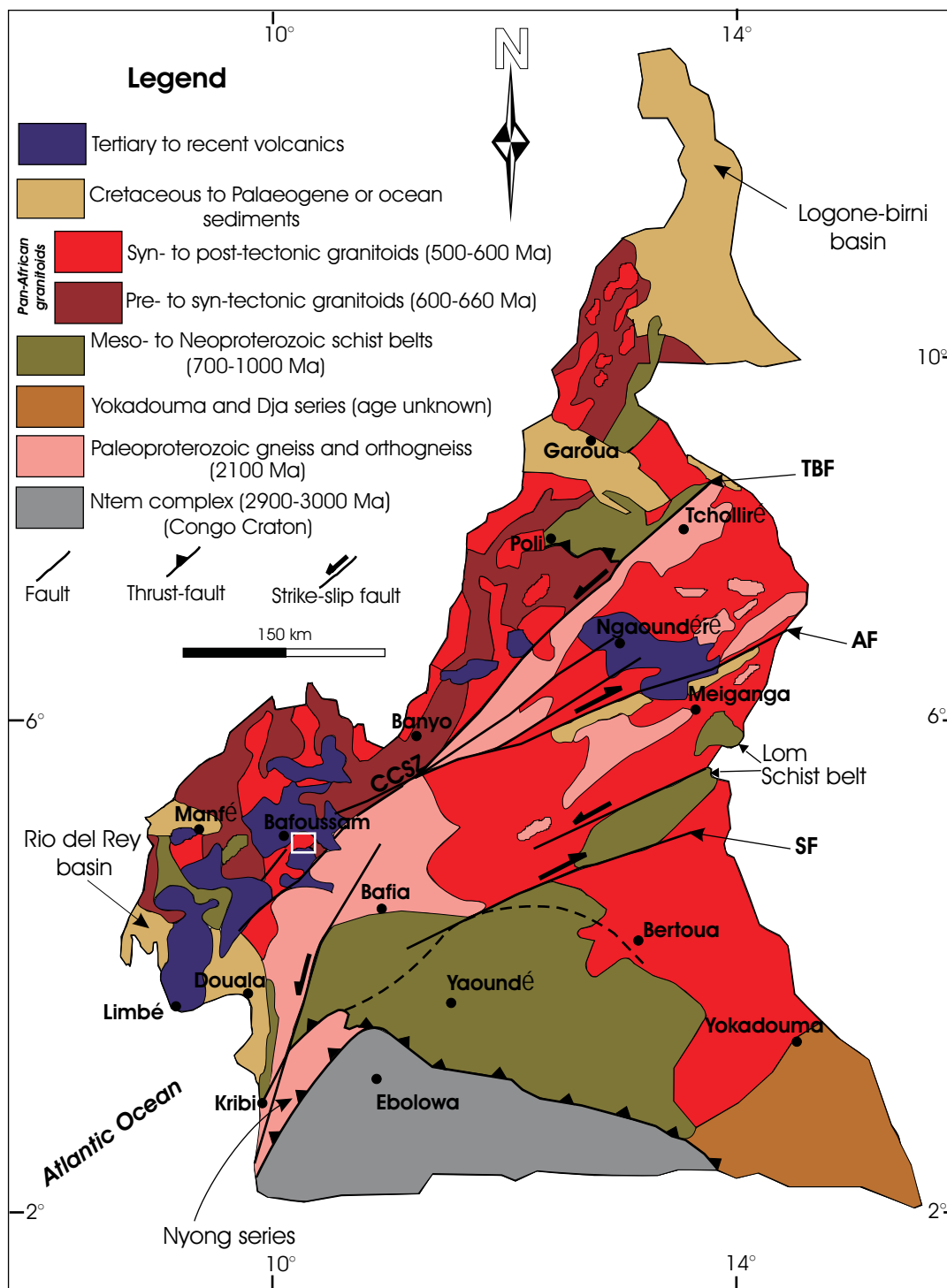


**Figure 1.4:** Geologic sketch map of Cameroon showing the main lithostratigraphic domains of the Neoproterozoic Pan-African orogenic belt, adapted from Soba et al. (1989) and Toteu et al. (2001). Note the general distribution of the large amount of Pan-African Granitoids; the three granitoid groups are not distinguished here because of the scale. TBF: Tcholliré-Banyo fault, AF: Adamaoua Fault, CCSZ: Central Cameroon Shear Zone, SF: Sanaga Fault. Dashed line represents the assumed geophysical limit of the Congo craton after Toteu et al. (2004). The location of study area is denoted by a heavy white outline.

It consists of strongly deformed metasedimentary rocks principally made up of migmatitic kyanite- and garnet-bearing gneisses, garnet-bearing schists and micaschists. Scarce dyke-like metaplutonic intrusions of garnet–pyroxene metadiorite qualified as *pyriclasite* by Nzenti et al. (1988) and chromitic/nickeliferous gabbro are also identified. The metasedimentary rocks yielded a Sm–Nd whole-rock and garnet age of 616 Ma, whereas the garnet–pyroxene metadiorite provided an age of  $620 \pm 10$  Ma using U–Pb on zircons (Penaye et al., 1993; Toteu et al., 1994). These ages are dating the Pan-African regional metamorphism which culminates in granulite facies. Rutile mineralization is widely dispersed through the Yaoundé schist belt and seems to be closely related to the Pan-African orogeny (Stendal et al., 2004).

The differences among these basins, particularly with respect to their rock types, may be a consequence of their location in relation to the Congo craton (Toteu et al., 2001): the Poli basin is distal, while the Yaoundé and Lom basins are more or less proximal. Similar basins have been identified within the Trans-Saharan fold belt in the Nigeria province where they are interpreted as marginal basins in response to the subduction that took place at the East of the West African Craton (Fitches et al., 1985; Caby et al., 2001).

### 1.1.2.3 Pan-African granitoids

The Pan-African granitoids intrude both the Paleoproterozoic gneissic basement and the Meso- to Neoproterozoic schist belts. Some of the granitoids were emplaced during an early stage of deformation and were then modified into orthogneisses at the later uplift stage of the geotectonic evolution. The Pan-African granitoids have classically been subdivided into three main generations, based on relation (discordance, concordance) between them and their host rock environment, and/or their structure and emplacement concordances or their intrusive and discordant character.

- ***Pre- to syn-D<sub>1</sub> granitoids*** are present throughout the Neoproterozoic orogenic belt and are particularly abundant to the west of the Tcholliré-Banyo fault (TBF: Fig. 1.4), in West Cameroon as well. In northern Cameroon, they include foliated granites, but also a basic to intermediate plutonic suite (BIP), dated at 630–620 Ma (U–Pb on zircons: Toteu et al., 1990). The BIP is mainly composed of calc-alkaline diorites, gabbros and granodiorites (Bassahak, 1988; Bassahak and Njel, 2004) with low  $^{87}\text{Sr}/^{86}\text{Sr}$  initial ratios (0.702–0.706). In West

Cameroon, granites and quartz-monzonites are dated at  $657 \pm 8$  Ma (Rb–Sr whole-rock isochron; Tagné-Kamga, 1994). Also related to this group are the charnockites from the Bandja massif, that have given an U–Pb zircons age of  $640 \pm 12$  Ma (Nguessi-Tchankam and Vialette, 1994)

- *Syn- to post-D<sub>2</sub> granitoids* include most of the granitoids of this study and occur in the Ngaoundéré region in the North, but also in West and in East Cameroon. They are mostly represented by anatectic granites, porphyritic granites and granodiorites of calc-alkaline to sub-alkaline composition. Syenitic and charnockitic plutons are also related to this group. To the North, anatectic granites are interpreted to derive from partial melting of an immature protolith with initial  $^{87}\text{Sr}/^{86}\text{Sr}$  ratios of 0.707 to 0.710. Large batholiths of porphyritic granites yielded U–Pb zircon ages between 600 and 580 Ma (Toteu et al., 1990). In West Cameroon, the region of the study area, high-K calc-alkaline granitoids gave ages varying between  $557 \pm 8$  and  $609 \pm 30$  Ma by the Rb–Sr whole-rock isochron method (Kwékam, 1993; Nguessi-Tchankam, 1994; Talla, 1995; Tagné-Kamga, 1994). Younger ages ranging from  $510 \pm 25$  Ma and  $552 \pm 10$  Ma derive from CHIME (Th–U–total Pb isochron method) on monazites (Tetsopgang, 2003). Recently, pseudorutile ( $\text{F}^{3+}_2\text{Ti}_3\text{O}_9$ ) has been locally found in these granitoids (Tetsopgang et al., 2003). Moreover, alkaline syenites from Banganté yielded ages of  $606 \pm 58$  Ma and  $630 \pm 35$  Ma (Rb–Sr whole-rock isochron: Tchouankoué, 1992). In the eastern part of Cameroon, Rb–Sr whole-rock isochron ages of  $614 \pm 41$  Ma and  $621 \pm 15$  Ma were obtained from S-type metagranites and anatectic granites, respectively, both originating from partial melting of immature sediments (Soba et al., 1991).

- *Post-orogenic granitoids* are dated, in North Cameroon, between  $546 \pm 9$  Ma and  $505 \pm 11$  Ma with initial ratios of  $^{87}\text{Sr}/^{86}\text{Sr}$  ranging between 0.706 and 0.712 (whole-rock Rb–Sr isochron ages: Lasserre et al., 1981a: b; Toteu et al., 1990). In south Cameroon within the Lom region, post-orogenic calc-alkaline granitoids gave whole-rock Rb–Sr isochron ages of  $491 \pm 4$  Ma and  $551 \pm 37$  Ma with high  $^{87}\text{Sr}/^{86}\text{Sr}$  initial ratios of 0.710–0.718 (Lasserre and Soba, 1976b). This group includes sub-circular plutons of dominantly alkaline composition, which are concentrated generally east of the Tcholliré-Banyo fault. Doleritic and microgranitic dykes are also related to this group.

According to their geographic position related to the Tholliré-Banyo fault (TBF: Fig. 1.4, Table 1.1 and 1.2) the Pan-African granitoids are further classified as follows (Toteu et al., 2001): (1) the Pan-African granitoids northwest of the fault are mainly orthogneissified and have

been considered to be originated from juvenile crust or crust with lesser amounts of older crustal component; and (2) the granitoid rocks southeast of the fault, in opposite, were emplaced after the main deformation ( $D_1$ ) and generated mainly by melting of the older (Eburnian) crust with limited juvenile inputs. The pre- to syn- $D_1$  granitoids occur exclusively in the northwest of the TBF, whereas the syn- to post- $D_2$  granitoids and the late orogenic granitoids are found in the both sides of the TBF (Fig. 1.4, Table 1.1 and 1.2).

#### 1.1.2.4 Tectonic evolution of the Neoproterozoic orogenic belt of Cameroon

Two main successive tectonic events were described in the entire Neoproterozoic orogenic belt of Cameroon (Nzenti et al., 1992; Toteu et al., 1990): (1) the  $D_1$  compressive deformation occurred during the peak of the Pan-African collision. To the north (Poli and Ngaoundéré regions), it is associated with an early medium- to high-pressure regional metamorphism, followed by intensive migmatization and emplacement of scarce plutonic rocks; and (2) the  $D_2$  deformation is dominated by N–S to NE–SW trending, steeply dipping strike-slip  $D_2$  foliations in the north (Poli and Ngaoundéré regions), while to the south (Yaoundé region) the E–W flat-laying  $D_2$  foliations are the result of southward-directed nappe thrusting. Intensive migmatization and emplacement of plutonic bodies are also related to the  $D_2$  deformation. These two main deformation phases are followed by the late Pan-African development of three main shear zones (see Fig. 1.4) which seem to be the result of horizontal movement following the multistage collision (Toteu et al., 2004).

- The ENE-trending *Tcholliré-Banyo fault* (TBF: Pinna et al., 1994) at the extreme North of Cameroon is believed to be the major boundary separating the Proterozoic orogenic belt of Cameroon in two parts: (1) an accreted juvenile Pan-African crust to the northwest; and (2) a large domain of remobilized Archean to Early Proterozoic continental margin to the southeast, i.e. north of the Congo craton (Pin and Poidevin, 1987; Nzenti et al., 1988).

**Table 1.1:** Available geochronological data for the Pan-African granitoids situated northwest to the Tcholliré-Banyo fault (TBF) within the Neoproterozoic belt of Cameroon. Locations with asterisk (\*) are in the vicinity of the Bafoussam area.

Age scale	Location	Alkalinity	$^{87}\text{Sr}/^{86}\text{Sr}$ (initial)	Material	Age (Ma) with method			Authors
					Rb – Sr	U – Pb	CHIME	
<b>Late orogenic</b>	Papata	alkaline	$0.7061 \pm 0.0008$	WR	$505 \pm 11$ Ma			Lasserre et al. (1981a)
	Godé	alkaline	$0.7089 \pm 0.0009$	WR	$516 \pm 06$ Ma			Lasserre et al. (1981a)
	Dogba	alkaline	$0.7077 \pm 0.0017$	WR	$519 \pm 07$ Ma			Lasserre et al. (1981a)
	Goutchoumi	alkaline	$0.7110 \pm 0.0142$	WR	$526 \pm 10$ Ma			Lasserre et al. (1981b)
	Anloa	alkaline	$0.7107 \pm 0.0026$	WR	$531 \pm 19$ Ma			Lasserre et al. (1981b)
	Makassa	alkaline	$0.7096 \pm 0.0220$	WR	$534 \pm 15$ Ma			Lasserre et al. (1981a)
<b>Syn- to Post D<sub>2</sub></b>	Nkambé *	calco-alkaline	–	monazite			510–552 Ma	Tetsopgang (2003)
	Bandja *	calco-alkaline	$0.7089 \pm 0.0003$	WR	$557 \pm 08$ Ma			Nguiessi-Tchankam et al. (1994)
	Fomopéa *	calco-alkaline	$0.7090 \pm 0.0003$	WR	$575 \pm 17$ Ma			Kwékam (1993)
	Batié *	calco-alkaline	$0.7077 \pm 0.0006$	WR	$576 \pm 24$ Ma			Talla (1995)
	Poli	calco-alkaline	–	zircon		600–580 Ma		Toteu et al. (1990b)
	Ngondo *	calco-alkaline	$0.7056 \pm 0.0018$	WR	$609 \pm 30$ Ma			Tagne-Kamga (1994)
Bangangté *	calco-alkaline	$0.7080 \pm 0.0006$	WR	$606\text{--}630$ Ma			Tchouankoué (1992)	
<b>Pre- to Syn D<sub>1</sub></b>	Poli	calco-alkaline	–	zircon		630–620 Ma		Toteu et al. (1990)
	Bakonwa	calco-alkaline	–	zircon		$633 \pm 03$ and $665 \pm 10$ Ma		Toteu et al. (2001)
	Bandja *	calco-alkaline	–	zircon		$640 \pm 12$ Ma		Nguiessi-Tchakam et al. (1994)
	Bangoua *	–	–	zircon		628 Ma		Toteu et al. (2001)
	Kumba-Manfé	calco-alkaline	$0.7080 \pm 0.0005$	WR	$655 \pm 30$ Ma			Lasserre et Soba (1979)
	Ngondo *	calco-alkaline	$0.7055 \pm 0.0001$	WR	$657 \pm 08$ Ma			Tagne-Kamga (1994)
	Manengouba	calco-alkaline	$0.7044 \pm 0.0002$	WR	$686 \pm 17$ Ma			Lamilen (1989)

**Table 1.2:** Available geochronological data for the Pan-African granitoids located southeast to the Tcholliré-Banyo fault (TBF) within the Neoproterozoic belt of Cameroon. Note the absence of the pre- to syn  $D_1$  Pan-African granitoids in this side of the fault.

Age scale	Location	Alkalinity	$^{86}\text{Sr}/^{87}\text{Sr}$ (initial)	Material	Age (Ma) with method Rb – Sr	Authors
<i>Late orogenic</i>	Nyibi	calc-alkaline	$0.7187 \pm 0.0010$	WR	$491 \pm 04$ Ma	Lasserre and Soba (1976b)
	Kongolo	alkaline	$0.7108 \pm 0.0002$	WR	$544 \pm 40$ Ma	Lasserre and Soba (1976b)
	Yaoundé	–	$0.7117 \pm 0.0009$	WR	$570 \pm 30$ Ma	Lasserre and Soba (1979)
<i>Syn- to post <math>D_2</math></i>	Ndokayo	subalkaline	$0.7670 \pm 0.0104$	WR	$614 \pm 41$ Ma	Soba et al. (1991)
	Kadei	subalkaline	$0.7137 \pm 0.0003$	WR	$621 \pm 15$ Ma	Soba et al. (1991)

- **The Central Cameroon Shear Zone (CCSZ:** Ngako et al., 1991; 2003), also called **Adamaoua fault (AF)**, is the most important lineament. It is a ductile fault trending N 70 °E which extends about 2000 km from Cameroon to the Gulf of Aden in Sudan (Browne and Fairhead, 1983; Cornacchia and Dars, 1983). Castaing et al. (1994), Vauchez et al. (1995) and Davison et al. (1995) have shown that the Central Cameroon Shear Zone is the continuation of the Northeast Brazil Pernambuco dextral transcurrent fault system on the African continent (PF: see Fig. 1.3B). Mylonitic outcrops related to this fault are widespread in the west part of Cameroon and within the study area, as well. According to Njonfang et al. (1998), the mylonitization took place in the deeper crust (15–20 km) under *T* and *P* conditions estimated at 730–800 °C and  $5 \pm 1$  kbar in West Cameroon.

- **The Sanaga fault (SF)**, identified by landsat remote sensing, corresponds to a major N 70 °E lineament in the north of the northern margin of the Congo Craton (Dumont, 1986). It strikes from Cameroon to the Central African Republic. Extensive outcrops of pseudotachylytes have been noticed along the Sanaga fault in south-west Cameroon and are considered as the result of the intense movements of this fault (Njom et al., 2004).

Available kinematical data (Browne and Fairhead, 1983; Ngako et al., 1991; Wilson and Guiraud, 1992) are consistent with a dextral movement along these shear zones during the late Pan-African orogeny. However, Archanjo and Bouchez (1991) in Brazil, and Ngako et al. (2003) in Cameroon voted for an earlier sinistral shear movement that was later followed by the dextral one.

### 1.1.3 Mesozoic to Tertiary sedimentary basins

The sedimentary basins in Cameroon resulted from the continental rifting of the South American and African plates during the opening of the South Atlantic Ocean at Early Cretaceous and Palaeogene times (Guiraud and Maurin, 1991; Guiraud et al., 1992). Two main sedimentary basin types are identified in Cameroon. They partly cover the Neoproterozoic orogenic belt. In northern Cameroon, the sedimentary facies is largely continental, while in the coastal zone in south Cameroon, it is mainly marine.

- **The coastal sedimentary basins** were formed when the South Atlantic Ocean invaded the older rift basins. They represent the significant liquid and gas hydrocarbon basins of

Cameroon. To the northwest is the offshore *Rio del Rey basin* (~ 7000 km<sup>2</sup>) located in Limbé, which is a southeastern extension of the Niger Delta system. To the southwest is the offshore and onshore *Douala/Kribi-Campo basin* along Cameroon's western coast. The latter basin covers an approximate total surface of 19000 km<sup>2</sup> of which 7000 km<sup>2</sup> are onshore and are part of the greater West African margin basin system. The Douala/Kribi-Campo basin comprises lower Cretaceous (ca. 140–120 Ma) sedimentary rocks which are interpreted to be immature submarine fans, lagoonal, fluvio-deltaic and alluvial deposits. The Douala/Kribi-Campo basin shows many similarities with the offshore Sergipe-Alagoas basin in eastern Brazil (Mayer et al., 1996).

- ***The intracratonic inland basins*** are also related to the separation of African and South America during the western Gondwana break-up. In the north of the country are the *Logone-Birni basin* (27000 km<sup>2</sup>) and the *Garoua basin* (6000 km<sup>2</sup>), and in the northwest is the *Mamfé basin* (3000 km<sup>2</sup>). The Garoua and Mamfé basins are the continuation of the Benue Trough in Nigeria (see Figs. 1.4 and 1.5). The intracratonic basins of Cameroon belong to the West and Central African rift systems. The deposits of the basins are essentially clays, fine-grained sandstones and conglomerates which correspond to the fluvial and lacustrine continental environment (Maurin and Guiraud, 1990). They include also some volcanic rocks (Ngounouno et al., 2003).

Petroleum exploration which began in the 1950's in Cameroon has been performed by several foreign oil companies. Exploration concentrated in the Rio del Rey and Douala/Kribi-Campo basins. The largest part of the production (80%) is exported, while the remaining portion is processed by Cameroon oil refining industry (SONARA). But the important reserve of natural gas discovered in the coastal sedimentary basins has not been explored yet. Furthermore, the exploration of the intracratonic basins has still to be carried out to confirm their petroleum potential.

#### **1.1.4 Tertiary to recent volcanics**

The Tertiary to recent volcanics in Cameroon belong to the so-called *Cameroon Volcanic Line* (CVL). The Cameroon Volcanic Line is a succession of horst and graben structures (Déruelle et al., 1987: 1991) which are marked by an alignment of oceanic as well as continental volcanic centres, and by anorogenic complexes extruding through the Neoproterozoic basement



formations and Cretaceous sedimentary rocks. It is an approximately Y-shaped zone that trends more or less in an NNE–SSW direction over a distance of 1600 km from the island of Annobón in the South Atlantic Ocean through south-western Cameroon to northeastern Nigeria and northwestern Cameroon (Fig. 1.5). Perhaps it is extending to the island of Saint-Helena to the West and to Tibesti to the East (Vincent, 1970).

The origin of the Cameroon Volcanic Line provoked very considerable research interest (see Déruelle et al., 1991 for a review), but it is still a subject under debate. Thus, no general agreement has yet been established for its precise origin. The most accepted hypotheses by now are those by Moreau et al. (1987) who proposed that the Cameroon Volcanic Line resulted from the rejuvenation of a Pan-African fracture zone (N 30 °E) at the beginning of the opening of the Atlantic Ocean and by Marzoli et al. (1999: 2000) for whom it is a “hotline” probably following a lithospheric crack (N 30 °E) tapping sub-lithospheric mantle.

#### 1.1.4.1 The anorogenic complexes

The anorogenic complexes (about sixty: Lasserre, 1978) occur only on the continental section along the Cameroon Volcanic Line. They contain a range of rock types from very basic through intermediate to acid and have both plutonic and volcanic facies. The anorogenic complexes are therefore termed *plutonic-volcanic anorogenic complexes* (Njonfang et al., 1992). The up to now investigated massifs (nearly 20, see asterisks in Fig. 1.5) are composed of gabbros, diorites monzonites, syenites and granites, and associated slightly younger volcanic rocks such as basalts, trachytes, phonolites and rhyolites (e.g., Jacquemin et al, 1982; Nana, 1988; Ngonge, 1988; Ghogomu et al., 1989; Njonfang et al., 1992).

Petrological and geochemical data of all the plutonic rocks reveal alkaline to hyper-alkaline characteristics with peraluminous or peralkaline affinities. Reported geochronological data (Rb–Sr, K–Ar and  $^{40}\text{Ar}$ – $^{39}\text{Ar}$  analyses) indicate lower Tertiary ages of 66–30 Ma for the Cameroonian anorogenic complexes (Lasserre, 1978; Cantagrel et al., 1978; Nguene, 1982; Caen-Vachette et al., 1991; Kamdem et al., 2002). The rocks of the anorogenic complexes were generated by partial melting of underlying continental crust and lithospheric mantle (Parson et al., 1986; Burke, 2001). There are only two mineralized anorogenic massifs known along the

Cameroon Volcanic Line, the Mayo Darlé to the North and Batcha to the West with Sn and Fe–Al–Ti ores, respectively.

The anorogenic complexes of Cameroon closely resemble in composition and in origin the anorogenic complexes of Jos Plateau in Nigeria called *Younger granites* (see Fig. 1.5: Tempier and Lasserre, 1980; Bowden et al., 1987) which intruded during late Jurassic between 213 and 141 Ma (Rahaman et al., 1984; Vail, 1989).

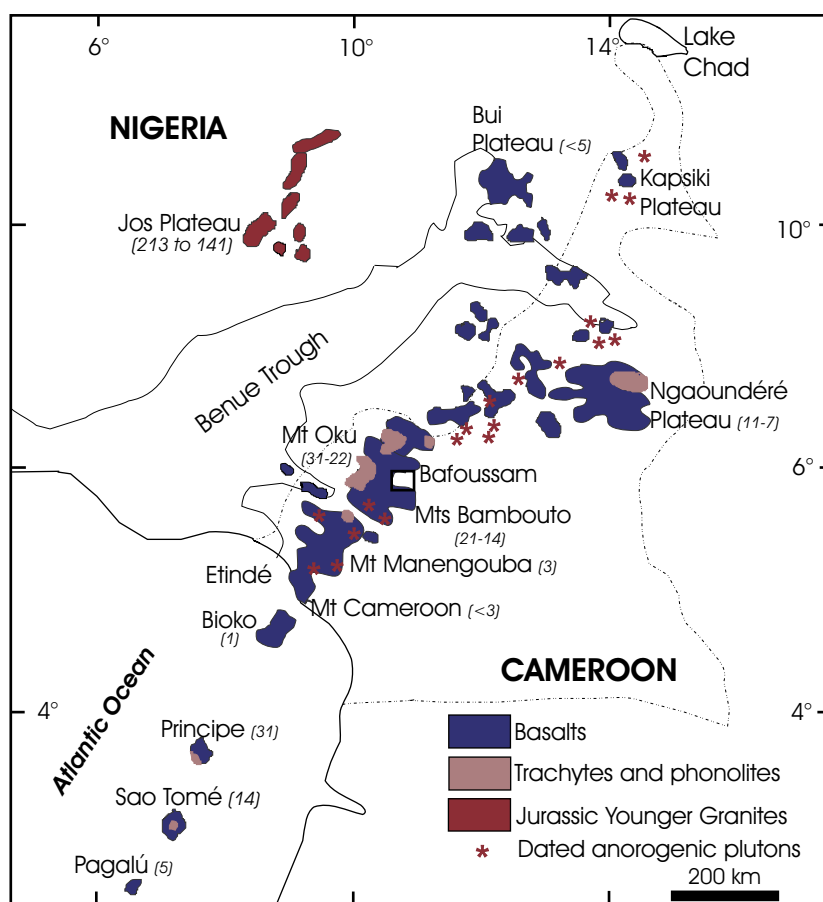


**Figure 1.5:** Sketch map of the Cameroon Volcanic Line showing oceanic and continental volcanic centres (blue and violet) and anorogenic complexes (asterisks); the Benue trough is also shown (adapted from Marzoli et al., 2000; Kamdem et al., 2002, number are ages in Ma according to Fitton and Dunlop, 1985). The outline delimits the study area.

#### 1.1.4.2 Volcanism

The volcanic centres are situated in both the oceanic and the continental section of the Cameroon Volcanic Line (see Fig. 1.5). They include four islands (Pagalú, formerly Annobon,

São Tomé, Príncipe and Bioko, formerly Fernando Poo), two seamounts, abundant continental volcanoes (e.g., Mont Etindé, Cameroon, Manengouba, Bambouto, Oku, Mandara) and over 35 crater lakes (e.g., lake Barombi-Mbo, Wum, Baleng, Monoun, Nyos), as well as the volcanic Plateaus Biu, Ngaoundéré and Kapsiki.

The current period of the volcanic activity started more or less 46 Ma ago and continues to present (K–Ar: Fitton and Dunlop, 1985;  $^{40}\text{Ar}$ – $^{39}\text{Ar}$ : Marzoli et al., 1999: 2000) through lavas emitted as flows and pyroclasts, and toxic gas ( $\text{CO}_2$ ) explosions issued from crater lakes. For example, Mount Cameroon (4090 m above sea level) on the ocean-continent boundary and the Monoun and Nyos cones are the active volcanoes along the Cameroon Volcanic Line. Within the last century, Mount Cameroon erupted seven times with the most recent eruptions in March 1999 and May 2000. Likewise, the crater lakes Lake Monoun (Sigurdsson et al., 1987) and Lake Nyos (Le Guern and Sigurdsson, 1989; Rice, 2000) released their poisonous gas ( $\text{CO}_2$ ) in 1984 and in 1986, respectively, which killed more than 1800 people.

The greatest volume of extruded rocks consists of basalt with subordinate amounts of more evolved phonolite and rhyolite compositions. Mineralogical and geochemical data show that the rocks belong to the alkaline series. The lavas of the oceanic as well as of the continental section exhibit indistinguishable geochemical and isotopic characteristics (Fitton, 1987; Halliday et al., 1988). A derivation from an asthenospheric mantle source has been suggested for the Cameroon Volcanic Line (Fitton and Dunlop, 1985; Halliday et al., 1988).

In the volcanic region of Cameroon, the lava flow rocks are extensively used for building trade and civil engineering (road-construction), while the ejecta from cinder cone are employed to improve agricultural techniques in lateritic soils. These volcanics are also processed by Cameroon's cement industry, CIMENCAM.

## 1.2 Aim of the study

The present study is focused on the granitoid rocks of the Bafoussam area that until now have not been investigated in any detail. Available geological information on the basement of this area is restricted to the regional reconnaissance study of Dumort (1968). Therefore, the

major objective of this study is to bring new elements into the comprehension of Pan-African magmatism in Cameroon as well as into the discussion relative to the palinstatic reconstitution between Central Africa and northeast Brazil, with regard to the genesis and geodynamic evolution of these granitoid rocks. This objective is achieved by the following constraints:

- (1) Detailed field studies and cartography help to identify the different granitoid rock types outcropping within the study area, their locations and extensions, and the relationships between the different rocks suites encountered. Macroscopic description enables a preliminary constraint on mineral composition of the sampled rock types with emphasis on the granitoid rock types for their subdivision.
- (2) Petrographical observation identifies and gives detailed description of all the minerals within each granitoid rock. The petrographic examination is also the basis of further investigations.
- (3) Mineral chemical investigations deal with the specific nature of major minerals from their chemical compositions and give some insights in the magma chemical evolution.
- (4) By using the mineral chemical data and with help of conventional geothermometer and geobarometer calibrations, the  $P$ - $T$  conditions of crystallization of the granitoids, as well as the oxygen fugacity ( $fO_2$ ) of their parent magmas are documented.
- (5) Geochemical investigations of the major-, trace- and rare earth elements help to assess the nomenclature the Bafoussam granitoids, to identify magmatic suites, to discriminate their tectonic setting and their genetic types, and to recognize the different processes involved during their evolution.
- (6) Isotopic data (whole-rock: Rb–Sr and Sm–Nd) provide the age of the granitoids and their emplacement in comparison with the Pan-African orogeny, and help for a further characterization of their magmatic sources as well.
- (7) Preliminary fluid inclusions investigations on hydrothermal quartz veins were performed in the order to describe the different types of fluid inclusions encountered, to determine their chemical compositions and to find a possible constraint of the conditions of the granitoids deformation.

## 2 GEOLOGY OF THE STUDY AREA

The study area, Bafoussam is rectangular-shaped and bounded by longitudes  $10^{\circ} 16' E$  and  $10^{\circ} 35' E$  and latitudes  $5^{\circ} 19' N$  and  $5^{\circ} 38' N$ . It stretches over an approximate surface of  $1000 \text{ km}^2$  (Fig. 2.1–2.2). The Bafoussam relief is made up by a of succession of valleys with 500–800 m of altitude, plateaus with an average altitude of 1400 m, and a positive topography with very steep hill slopes and volcanoes (about 2000 m of altitude).

Geologically, the Bafoussam area is part of the Cameroon Neoproterozoic orogenic belt, located along the southern extension of the Central Cameroon Shear Zone (CCSZ: Fig. 1.5) as well as on the great axis of the Cameroon Volcanic Line (CVL: Fig. 1.6). The Bafoussam area rocks consist of migmatitic gneiss country-rocks which are intruded by granitoid rocks of varied compositions; both gneissic and granitoid rocks are in places covered by Tertiary volcanic rocks (Fig. 2.2).

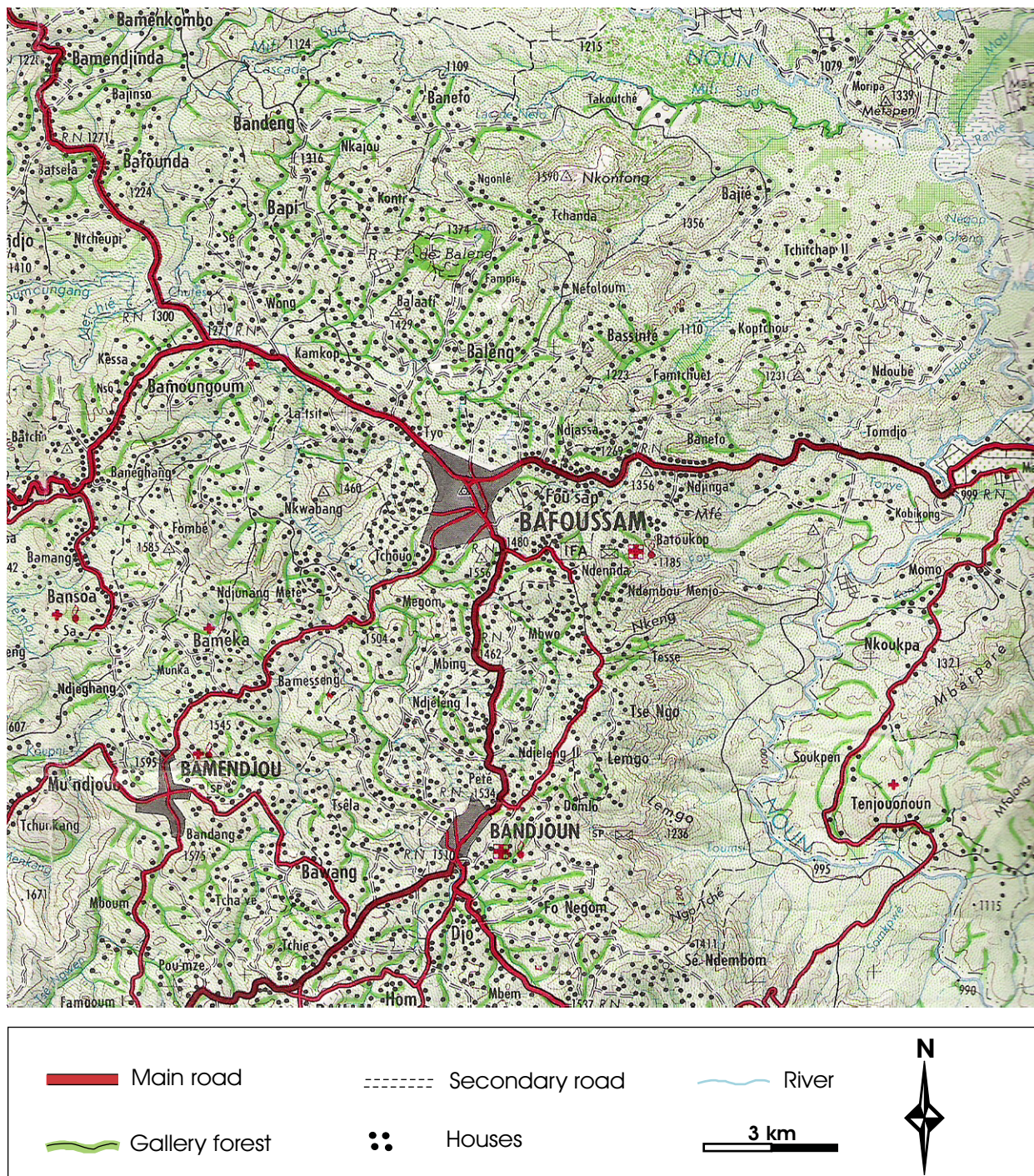


**Figure 2.1:** Topographic map of the Bafoussam area, taken from the map 1:200,000 BAFOUSSAM (sheet NB-32-XI) (1978) drawn and published by the National Geographic Centre, Yaoundé.

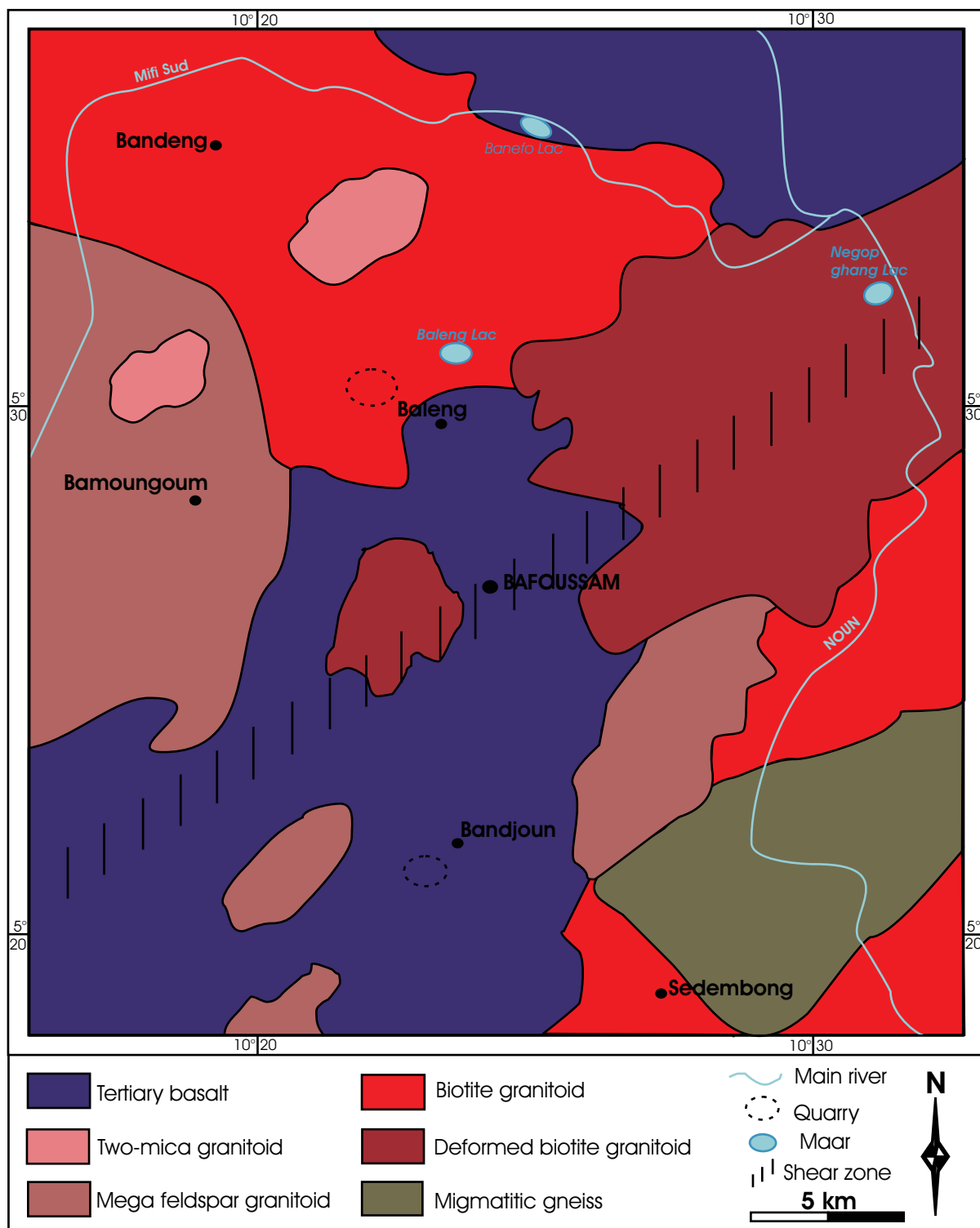


**Figure 2.2:** Generalized geological map showing the distribution of the individual types of granitoid rocks, associated migmatitic gneiss country-rocks and the Tertiary basalt within the Bafoussam area.

## 2.1 Metamorphic rocks: migmatitic gneiss and amphibolite

*Migmatitic gneiss* is located at the southeast part of the study area. It is observed eastward, along the road-cut near the bridge of the river Noun (Fig. 2.3A) or occurs as isolated flagstones near Sedembong locality (Fig. 2.3B, C). It is light grey coloured, fine- to medium-grained and granoblastic, displaying a regular decimetric to centimetric layering. Dark, biotite-rich layers alternate with white quartzofeldspathic layers. These layers are broadly directed SSE–NNW and are locally folded on a centimetre- to decimetre scale with the axial planes of the folds subparallel to the main foliation (Fig. 2.3D, E and F).

Rare *amphibolite* bodies are locally observed as country rocks, intimately associated with the granitoids. The amphibolite consists mainly of green amphibole and plagioclase with little quartz. Hornblende-bearing and metagabbro enclaves have been also observed in these rocks. The metagabbro is a dark green and coarse-grained granoblastic rock and is composed of prominent large crystals of hornblende with crystal cores exhibiting a pigmentation of minute clinopyroxene relicts, plagioclase and opaque minerals, together with a minor amount of biotite and traces of quartz.

## 2.2 Granitoid rocks

The granitoid rocks are the most abundant petrographic type in the study area and occur mainly on hill slopes or along river-cuts. In outcrops, they are scattered among the area, commonly as isolated boulders and as flagstones of various shapes and sizes, or they form dome-like morphology reliefs through the widespread lateritic cover (Fig. 2.4A, B, C and D). Some granitoid bodies exhibit scale-like structures on their surface, which are believed to be signs of alteration; the size of the scales varies with the intensity of alteration (Fig. 2.4E, F).



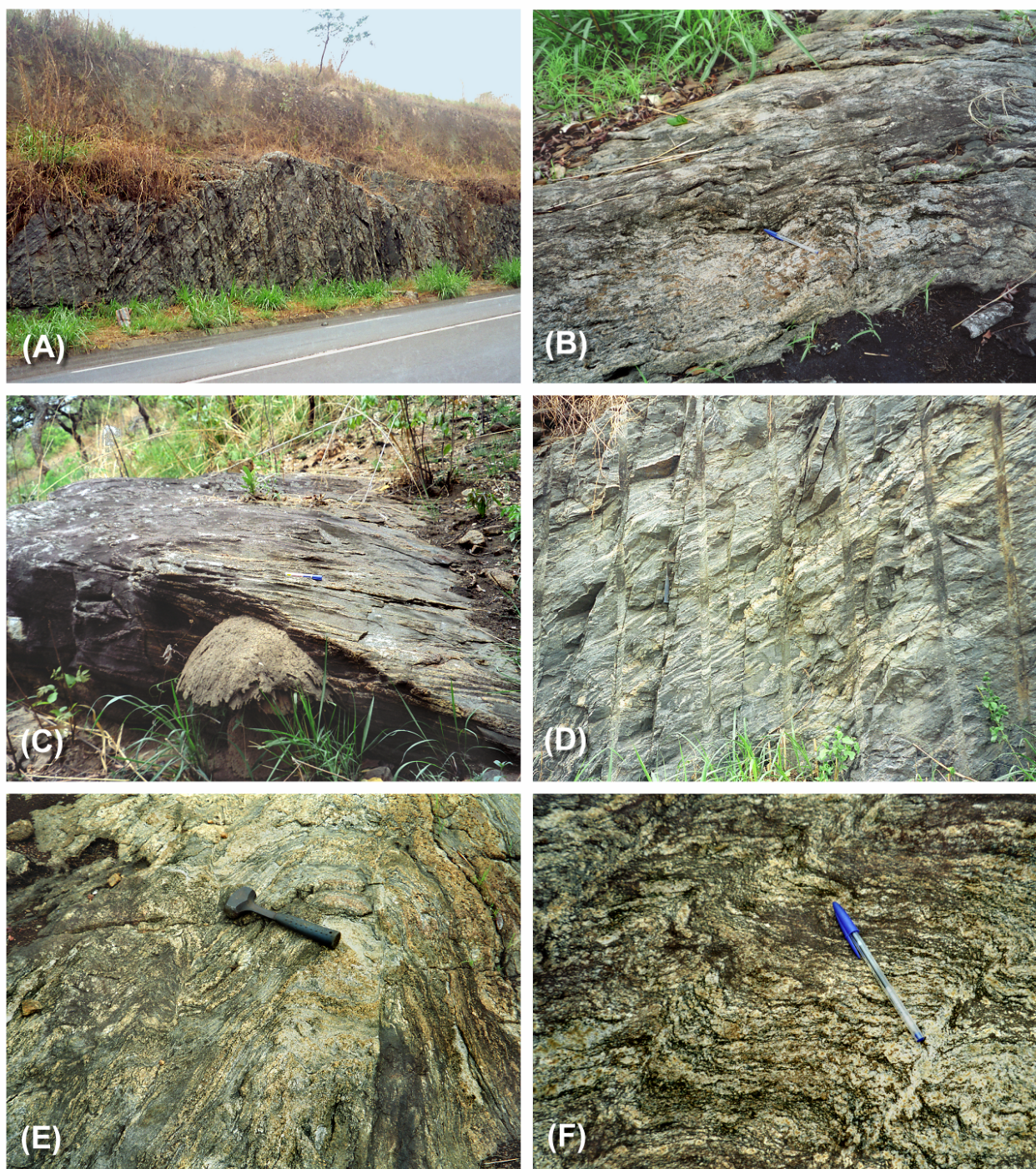


**Figure 2.3:** Field photographs of the migmatitic gneiss outcrops of the investigated area showing alternating micaceous and quartzofeldspathic layers. **(A)** Road-cut outcrop near the bridge of the river Noun (Locality:  $L = 10^{\circ} 33' 9''$ ,  $1 = 5^{\circ} 28' 48''$ ). **(B)** and **(C)** Flagstones (Sedembong locality:  $L = 10^{\circ} 30' 28''$ ,  $1 = 5^{\circ} 26' 17''$  and  $L = 10^{\circ} 29' 7''$ ,  $1 = 5^{\circ} 20' 36''$ , respectively). **(D)** and **(E)** different folding within the migmatitic gneiss (Sedembong locality:  $L = 10^{\circ} 30' 28''$ ,  $1 = 5^{\circ} 26' 17''$ , for the both pictures).

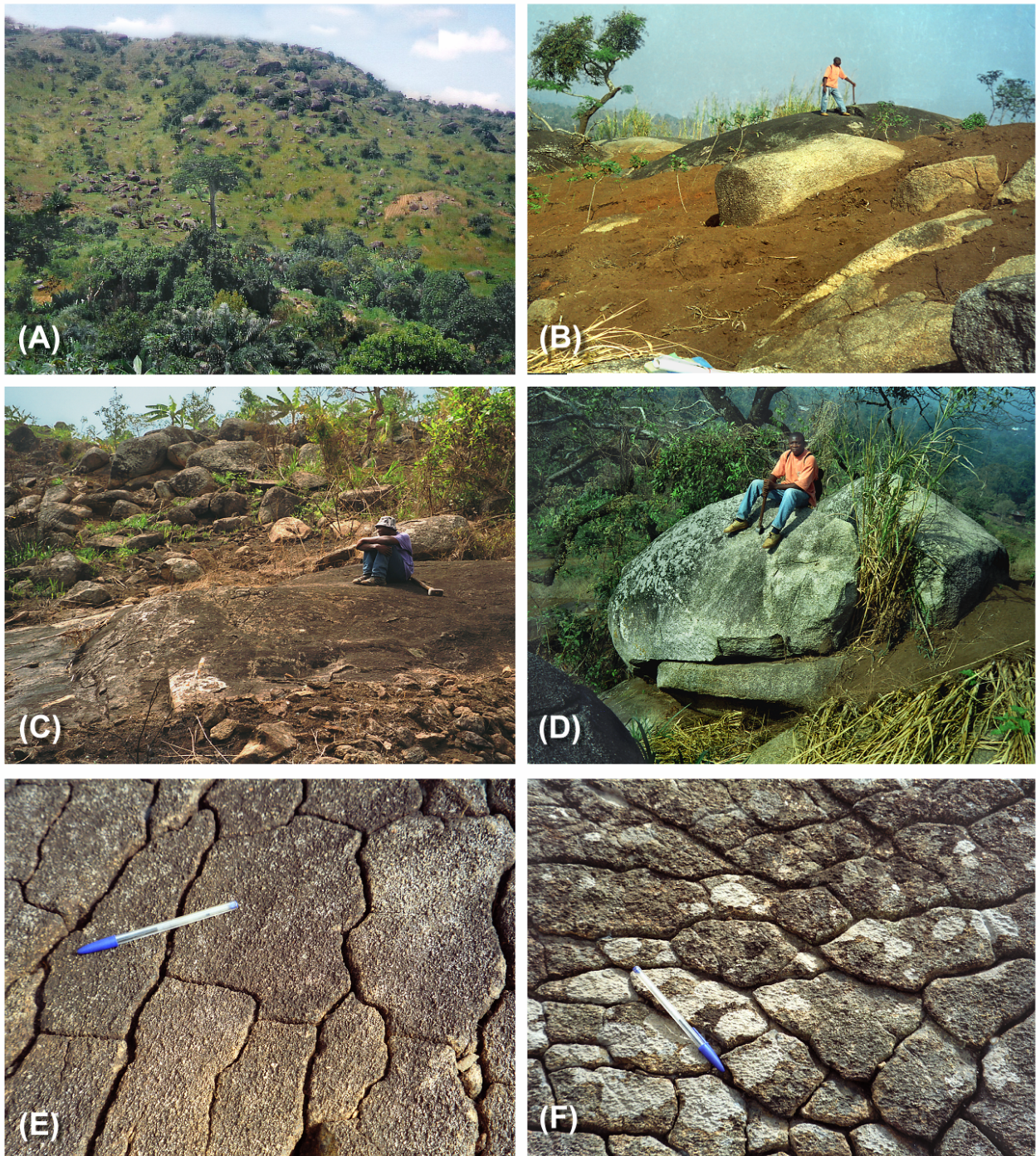


**Figure 2.4:** Field photographs of the studied granitoid outcrops. (A), (B), (C) and (D) Different shapes of the granitoid outcrops exposed elsewhere within the research area. (E) and (F) Granitoid rock outcrops displaying scales-like surfaces due to the alteration (Bamoungoum locality); the scales sizes are gradually reduced with the increase of alteration intensity.

The granitoid rocks have various compositions and based on their lithological features, they have been subdivided into four types, as following:

- (1) Biotite granitoid
- (2) Deformed biotite granitoid
- (3) Mega feldspar granitoid
- (4) Two-mica granitoid

### 2.2.1 Biotite granitoid

Biotite granitoid crops out in the northwest, Baden, Bapi and Baleng quarry, as well as along the south-eastern border (Sedembong locality) of the study area. It often occurs also as strips up to 30 cm wide crosscutting the deformed biotite granitoid bodies. These strips are generally elongated following the N 70 °E direction. The geological contact of the biotite granitoid with migmatitic gneiss is discordant. It is expressed by the difference in orientation between the biotite granitoid band (Fig. 2.5).

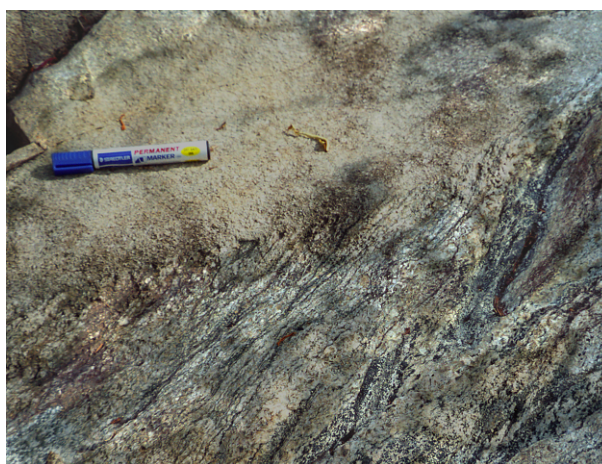


**Figure 2.5:** Field photograph of the biotite granitoid in contact with the migmatitic gneiss wall-rock. The migmatitic gneiss exhibits a strong foliation marked by mineral alignment (Sedembong locality: L = 10° 30' 28'', l = 5° 26' 17'').

The biotite granitoid is massive, whitish to light-grey colored and medium- to coarse-grained (up to 1 cm), having heterogranular texture with lack of preferred orientation. In places, a gradational change to rather a fine-grained, aplitic granitoid is observed. Two biotite granitoid subtypes can be distinguished. The first group contains only biotite whereas the other has biotite and amphibole as ferromagnesian minerals. But hereafter the two biotite granitoid subtypes are

taken separately only if necessary. The both subtypes are additionally composed of quartz and feldspars.

The biotite granitoid usually contains hornblende-bearing enclaves of different sizes, either elongated or lenses-like in shape (Fig. 2.6A, B). Late aplite, pegmatite and quartz dykes are observed in several thicknesses (millimetres to centimetres), crosscutting the biotite granitoid bodies, often together with amphibolite enclaves (Fig. 2.6A, B and C). In the Baleng quarry, some pegmatite dykes exceptionally contain garnet, pyrite, green beryl and molybdenite. The pegmatite dyke is locally transected and displaced following a sinistral shear movement by the aplite dyke, indicative of its earlier emplacement (Fig. 2.6D). Moreover, several fault systems, chiefly subvertical and NE–SW-trending, crosscut the biotite granitoid (Fig. 2.6 E, F). The faults are sometimes filled by a dark green coloured rock (phylionite?) of about 14 cm in width (Fig. 2.6F), as exposed in the Baleng quarry. This rock is strongly foliated and consists of pink potassium feldspar porphyroclasts in a matrix of minute minerals, principally amphibole, quartz and biotite which are indistinguishable by naked eye.

### **2.2.2 Deformed biotite granitoid**

The deformed biotite granitoids form a band of about ~ 6 km thickness that occurs from the centre part of the study area to the Northeast, observed in Bafoussam town and near Baleng locally, respectively. It broadly stretches ENE–WSW, parallel to the Central Cameroon Shear Zone, and is considered as its south-west extension. The deformed biotite granitoid exhibits various degrees of deformation mainly noticed at the grain scale and can be therefore referred to as a mylonite based on the intensity of the granulation, according to Berthé et al. (1979) and Passchier and Trouw (1998). The contacts between the deformed biotite granitoid and the biotite granitoid are: (1) concordant, depicted by the parallelism between the mylonitic schistosity in the deformed biotite granitoid and the elongation of the biotite granite strip (Fig. 2.7A, B); and (2) discordant, portrayed by different orientation of the deformed biotite granitoid schistosity and the biotite granitoid strip (Fig. 2.7C).



**Figure 2.6:** Outcrop photographs of the biotite granitoid. **(A)** Biotite granitoid with hornblende-bearing lenses-like shaped enclaves, both transected by an aplite dyke (location northward to Sedembong locality:  $L = 10^{\circ} 33' 09''$ ,  $l = 5^{\circ} 28' 48''$ ). **(B)** Elongated hornblende-bearing enclaves cross-cut by aplite and quartz dykes of different generations (Baleng quarry:  $L = 10^{\circ} 23' 47''$ ,  $l = 5^{\circ} 31' 27''$ ). **(C)** Large pegmatite dyke (25 cm) in a biotite granitoid. **(D)** Late aplite dyke ( $N 15^{\circ} E 65^{\circ} W$ ) cross-cutting an earlier pegmatite dyke ( $N 146^{\circ} E 52^{\circ} SW$ ) (Sedembong locality:  $L = 5^{\circ} 20' 23''$ ,  $l = 10^{\circ} 29' 8''$ ). **(E)** Pegmatite dyke cross-cut by a fault ( $N 40^{\circ} E$ ) (Badeng locality:  $L = 10^{\circ} 22' 32''$ ,  $l = 5^{\circ} 34' 54''$ ). **(F)** Fault ( $N 17^{\circ} E$ ) filled by a dark green coloured rock (phylonite?) of about 14 cm in width (Baleng quarry:  $L = 10^{\circ} 23' 47''$ ,  $l = 5^{\circ} 31' 27''$ ).

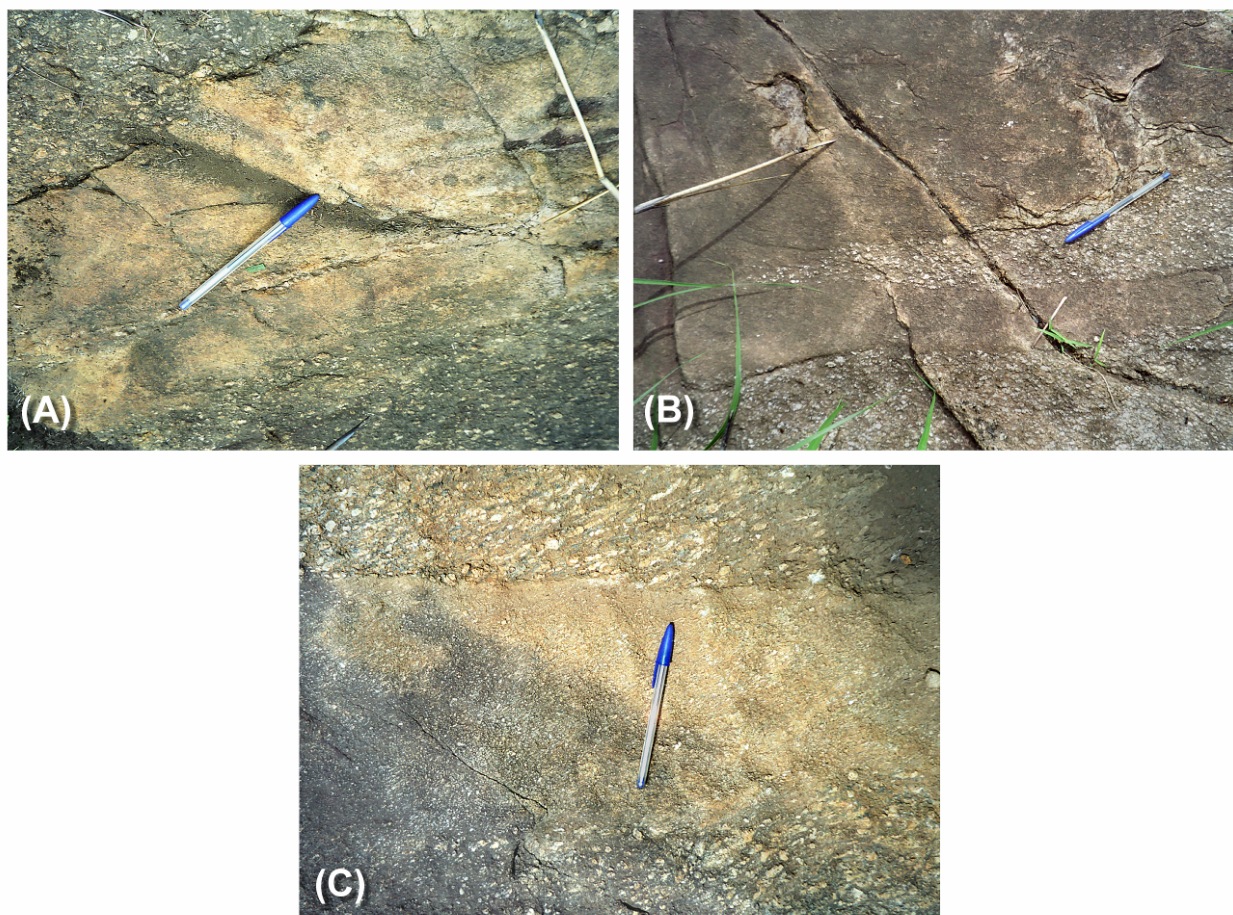


**Figure 2.7:** Outcrop photographs of the deformed biotite granitoid in contact with the biotite granitoid. **(A)** Concordant contact between deformed biotite granitoid and biotite granitoid (Eastward Baleng quarry: L = 10° 28' 22'', l = 5° 34' 47''). **(B)** Interpenetration of the deformed biotite granitoid in the biotite granitoid strip (Eastward Baleng quarry: L = 10° 28' 22'', l = 5° 34' 47''). **(C)** Discordant contact between deformed granitoid and biotite granitoid (Bafoussam town: L = 10° 23' 58'', l = 5° 29' 27'').

The deformed biotite granitoid is mesocratic, heterogranular and has predominantly granoblastic texture. It is characterised by large porphyroclasts (1cm x 5 mm) of white potassium feldspar embedded in a relatively fine-grained groundmass of plagioclase, quartz, biotite and locally amphibole (Fig. 2.8A, B, C and D). The preferred alignments of minerals are roughly NNE–SSW and NE–SW oriented. Like biotite granitoid, the deformed biotite granitoid can be subdivided into two subtypes, one having solely biotite whereas the other contains biotite and amphibole as ferromagnesian minerals. Hereafter, the two deformed biotite granitoid subtypes are specified when needed.

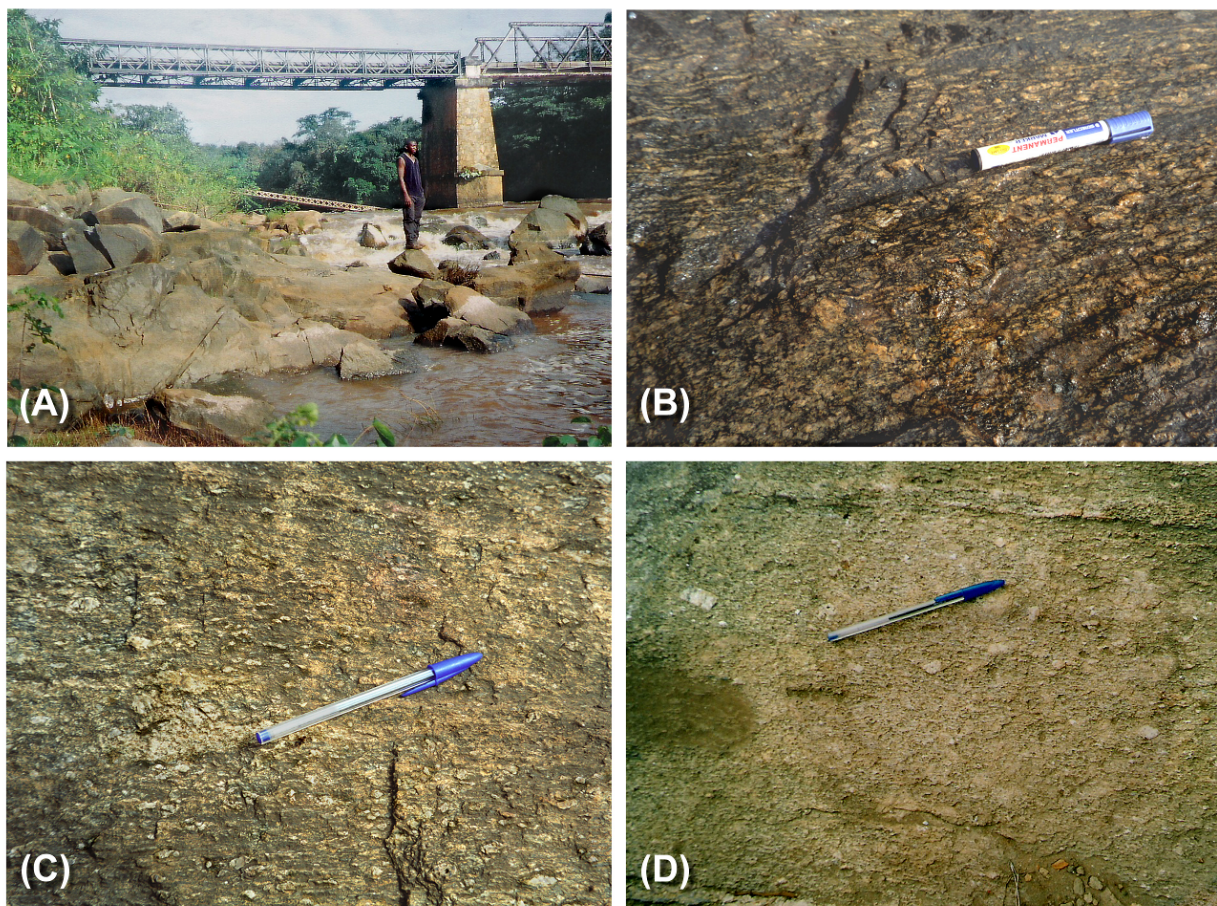


**Figure 2.8:** Field photographs of the deformed biotite granitoid. (A) An outcrop of the deformed biotite granitoid in river Noun-cut ( $L = 10^{\circ} 33' 23''$ ,  $l = 5^{\circ} 28' 29''$ ). (B), (C) and (D) Augengneiss texture in the deformed biotite granitoid with K-feldspar porphyroclasts embedded in a mylonitic groundmass. The K-feldspar porphyroclasts mode decreases from (B) to (D) [(B) from the river Noun-bed, (C) and (D) Eastward of Baleng:  $L = 10^{\circ} 29' 15''$ ,  $l = 5^{\circ} 32' 55''$ ].

The deformed biotite granitoid contains isolated enclaves of metagabbro of various shapes and sizes (Fig. 2.9A, B) with the most developed enclaves within the outcrops along the river Noun-cut (Fig. 2.8A). It also hosts locally dark green, strong foliated rocks (phyllonites?) similar to those filling the faults transecting the biotite granitoid in the Baleng quarry (Fig. 2.9C).

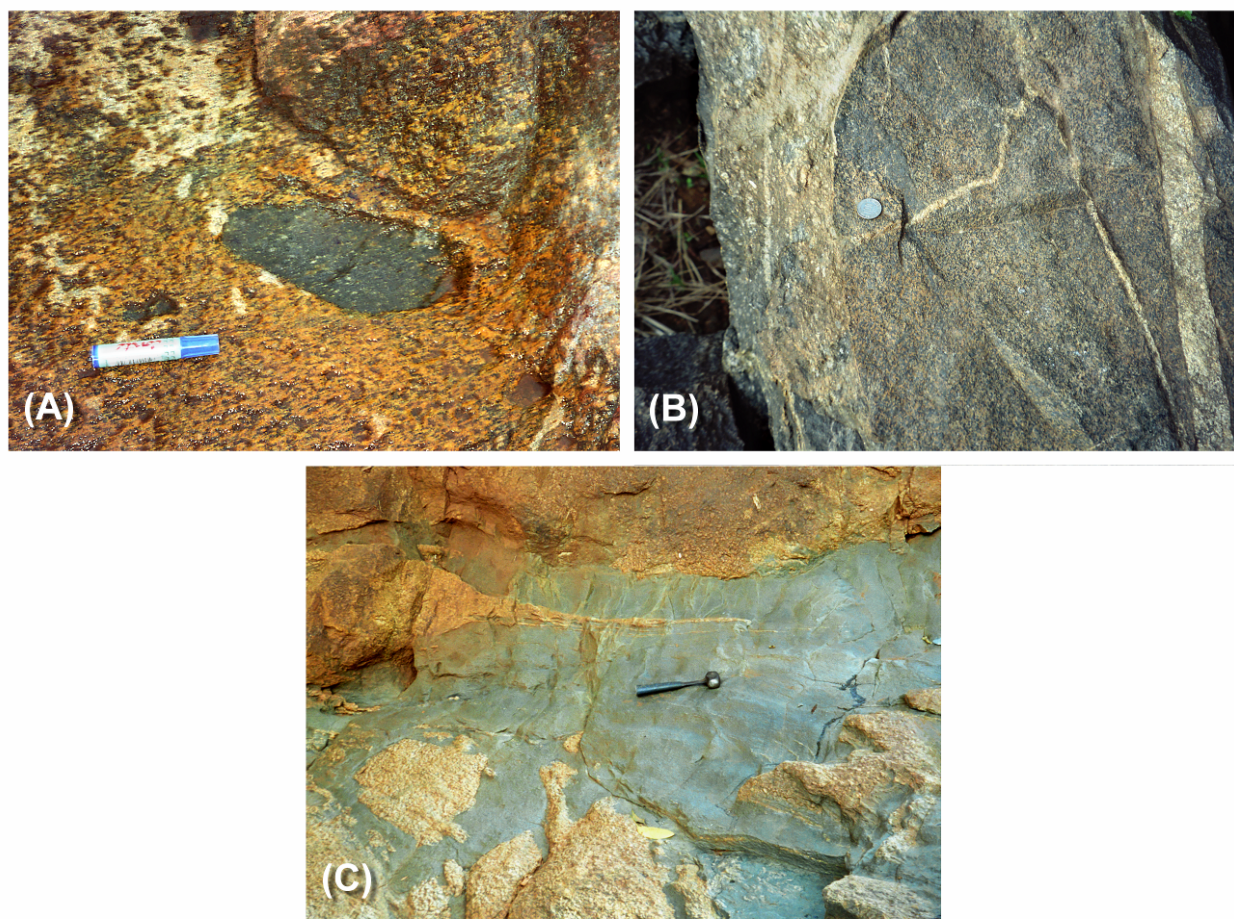


**Figure 2.9:** Outcrop photographs of the deformed biotite granitoid. **(A)** Isolated centimetre-scaled angular enclaves of metagabbro in a deformed biotite granitoid (small river-cut in Bafoussam town: L = 10° 23' 58'', 1 = 5° 29' 27''). **(B)** Large metagabbro enclave in deformed biotite granitoid (river Noun-cut: L = 10° 63' 23'', 1 = 5° 28' 29''). **(C)** Deformed biotite granitoid hosting strong foliated rock (phyllonite?) (small river-cut in Bafoussam town: L = 10° 23' 58'', 1 = 5° 29' 27'').

### 2.2.3 Mega feldspar granitoid

The mega feldspar granitoid occupies large parts of the Bamoungoum locality in the north-west, whereas it appears only in limited distribution in the southern part of the study area. However, as the south-western region of the study area is widely covered by lateritic soil from Tertiary volcanic rocks, a more widespread subsurface occurrence of the mega feldspar granitoid is possible. The relationship between the mega feldspar granitoid and the biotite granitoid is in places exposed, illustrated by a sharp contact between the two groups (Fig. 2.10).





**Figure 2.10:** Field photograph of the mega feldspar granitoid in sharp contact with the biotite granitoid. (Sedembong locality: L = 10° 28' 28'', l = 5° 26' 30'').

The mega feldspar granitoid is grey coloured and has a porphyritic texture. The outcrops are largely composed of large grains of white and pink potassium feldspar (2–6 cm long) being surrounded by a fine- to medium-grained matrix of quartz, feldspars and biotite flakes. The K-feldspar megacrysts are often sub-rectangular to rectangular in shape, some exhibiting symmetrical to dissymmetrical carlsbad twinning and/or optical and concentric zonation. The distance between the megacrysts is variable and they locally display a flow texture, roughly directed SSE–NNW. A gradational increase of the grain size of K-feldspar is observed from the north-west to the south of the study area (Fig. 2.11A, B and C).

To the south, the mega feldspar granitoid shows various degrees of deformation which is more or less absent in the north-western part of the area. This indicates that the melting of the mega feldspar granitoid might have been occurred syn- to post-tectonically, in which case the north-west part remained rigid. The deformation processes induced: (1) reduction of the density of K-feldspar megacrysts as well as their grain size (Fig. 2.11D); (2) modification of the K-feldspar megacrysts shape into lenses-like porphyroblasts, showing both sinistral and dextral shear senses without change of the original K-feldspar grains orientation (Fig. 2.11E); and (3) transformation of magmatic porphyritic texture into typical augengneiss texture defined by K-feldspar porphyroblasts wrapped by a mylonitic groundmass, reflecting a higher degree of deformation (Fig. 2.11F).

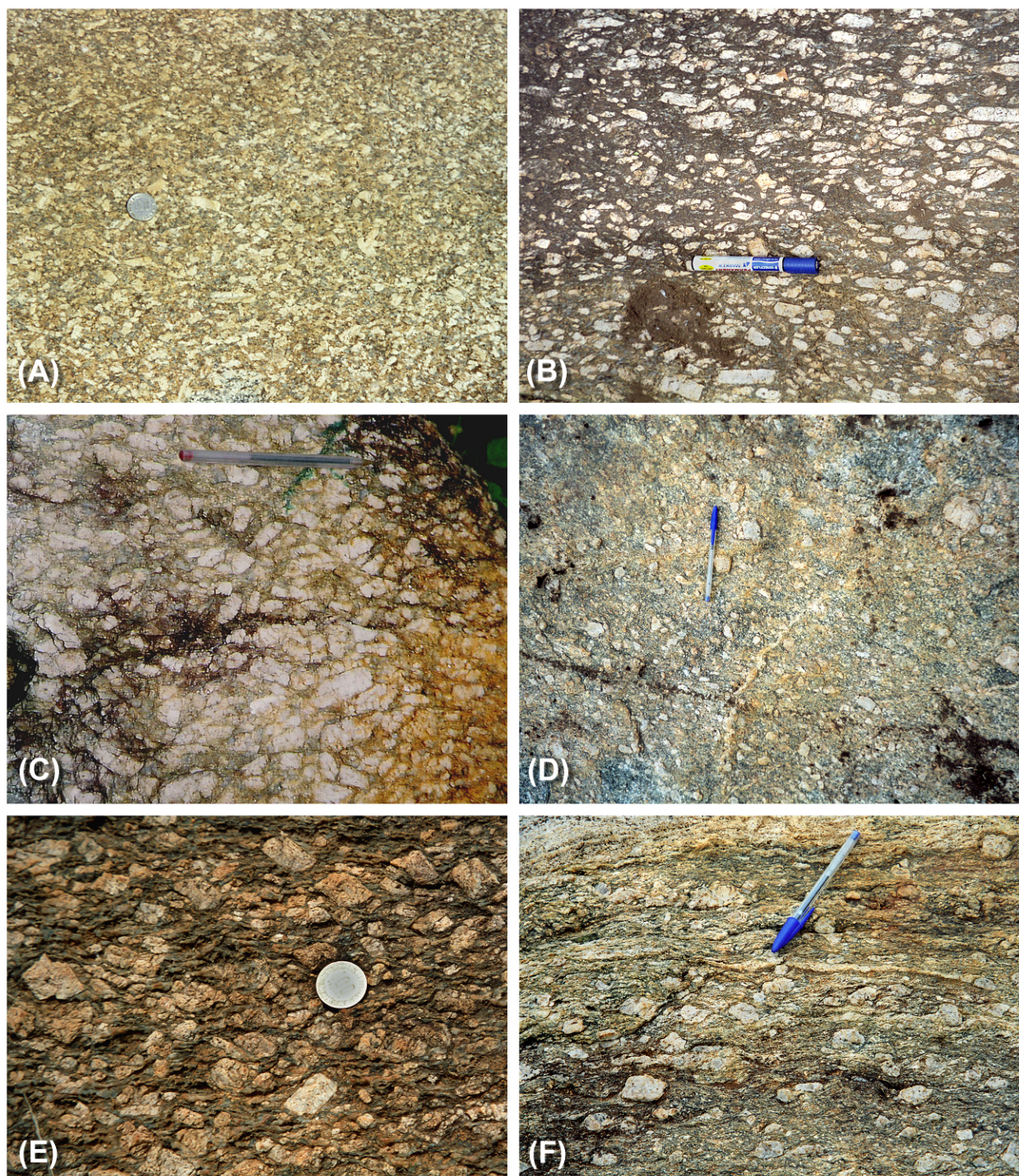


**Figure 2.11:** Outcrop photographs of the mega feldspar granitoid. (A), (B), and (C) Mega feldspar granitoid with a porphyritic texture defined by K-feldspar megacrysts showing a gradational increase of size from (A) to (C), embedded by a fine-grained matrix (Bamoungoum and Sedembong localities). (D), (E) and (F) Deformational signs in mega feldspar granitoid with in (E) and (F) augengneiss texture defined by K-feldspar porphyroblasts wrapped by a mylonitic groundmass [Bandjoun locality: L = 10° 28' 28'', l = 5° 26' 30'' for (D) and (F); L = 10° 23' 10'', l = 5° 23' 10'' for (E)].

### 2.2.4 Two-mica granitoid

The two-mica granitoid is of limited distribution within the study area, having the less representative outcrops. It is sporadically exposed in the north-west part, around Bamoungoum as massive, nearly homogeneous rocks. The contact relationships between the two-mica granitoid and the mega feldspar granitoid and the biotite granitoid are not completely understood. Since the two-mica granitoid exhibits little signs of deformation compared to other granitoids.

The two-mica granitoid is leucocratic and medium-grained. It is equigranular and essentially consists of feldspars and quartz with minor biotite, muscovite and some times garnet. The two-mica granitoid contains biotite-rich surmicaceous enclaves, having various sizes and shapes. Generally, these enclaves are composed of abundant biotite and subordinate feldspars, and occur in elongated shape, with their long dimensions broadly aligned parallel to the schistosity in the host granitoid (Fig. 2.12).

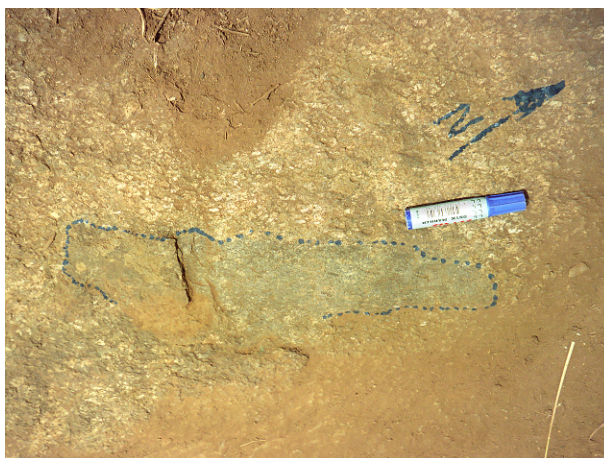


**Figure 2.12:** Outcrop photographs of the two-mica granitoid hosting a biotite-rich micaceous enclave having elongated shape (Bamoungoum locality).

### 2.3 Volcanic rocks

The volcanic activity of the Bafoussam area started with fissure eruption emitting enormous lava flows and continued by explosive episodes.

- *The Lava flows* are represented by basaltic trapps or plateaus, lying inconsistent upon the crystalline basement. The basaltic trapps are exposed only in places such as the quarry Bandjoun where they are structured in columnar jointing (Fig. 2.13A) and along river cuts where they are mainly exposed as blocks. Elsewhere, widespread lateritic red soils are formed at their expense. The lava flows are dominantly of pahoehoe type, and have been emplaced during the early activity of the Cameroon Volcanic Line ranging in age from 46 to 14 Ma (K–Ar: Fitton and Dunlop, 1985;  $^{40}\text{Ar}$ – $^{39}\text{Ar}$ : Lee et al., 1994; Marzoli et al., 1999). Tchoua (1974) and Déruelle et al. (1987) related this first volcanic activity to the reworking of the major faults and fractures along the Cameroon Volcanic Line main axis, N 30 °E. The rocks are solely aphyric alkaline basalts that sometimes exhibit cavities hosting calcite.

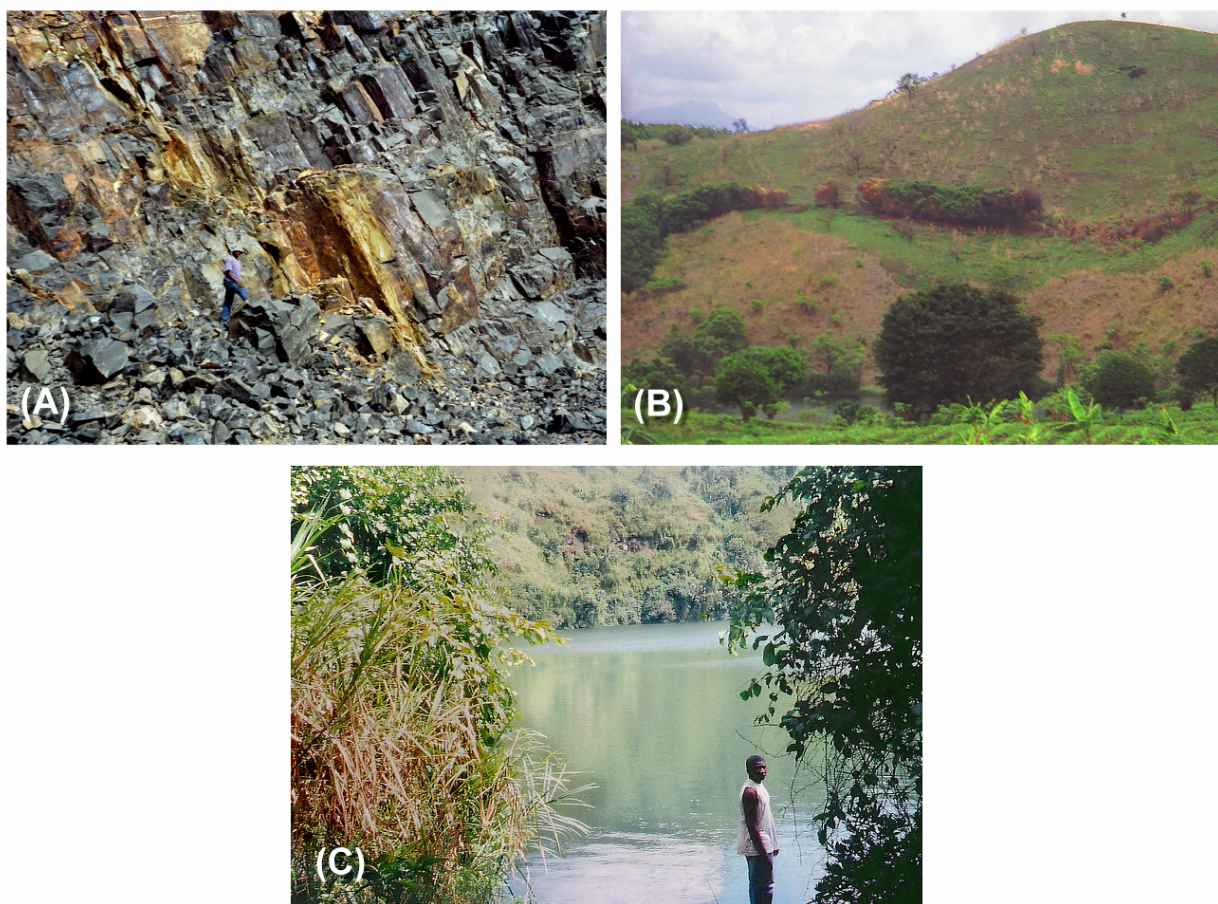


**Figure 2.13:** Field photographs of the volcanism-related environments. **(A)** Basaltic trapps with a typical columnar jointing structure in Bandjoun quarry. **(B)** Negop-ghang Lake built within volcanic rocks ( $L = 10^{\circ} 33' 34''$ ,  $l = 5^{\circ} 32' 42''$ ). **(C)** Baleng Lake built within granitoid rocks.

- *The explosive episode* that represents the late activity of the Western Highlands has been dated at 15–4 Ma ( $^{40}\text{Ar}$ – $^{39}\text{Ar}$ : Marzoli et al., 2000). It has generated three maar lakes (Baleng, Banefo and Negop-ghang Lakes) and cinder cones around Baleng, northward of the study area (Fig. 2.13 B, C). These volcanic cones are aligned N 30°E, directly reposed either on the older volcanics (lava flows) or on the migmatitic gneiss and granitoid rocks. They are built up by the aggregation of volcanic ejecta (lapilli, ash, blocks and bombs), xenoliths of basement rocks and lava flows. The volcanic activity has been recognized to be mildly explosive.

To conclude, the Bafoussam granitoids emplacement was chiefly controlled by the N 30°E shear zone in the prolongation of the Cameroon Volcanic Line (CVL), but also by the N 70°E Central Cameroon Shear Zone (CCSZ). In the field, these two directions are expressed in the schistosity and foliation trajectories, faults orientation and the alignment of the volcanic cones as well. This is in concordance with the results of detailed structural analysis in the area and adjacent regions (Njiekak et al., 2003) and the main deformation strikes within the Pan-African orogenic belt between the Congo craton and the West African craton (Njonfang et al., 1998; Ferré et al., 2002; Ngako et al., 2003).